Table 1: Baseline characteristics of patients.

Variable	Total ($n = 82$)	GLP-1 group ($n = 26$)	DPP-4 group ($n = 36$)	Pioglitazone group ($n = 20$)	P
Mean follow-up period (days)	520 (222–410)	342 (291–392)	250 (187–233)	1236 (378–2216)	<0.01‡
Age* (years old)	54.2 (44.4–63.2)	55.7 (50.2–62.3)	54.0 (42.7–64.3)	52.7 (46.3–59.6)	0.71†
Male, n (%)	61 (74.4%)	18 (69.2%)	29 (80.6%)	14 (70.0%)	0.55‡
Body weight* (kg)	80.7 (69.1–89.7)	81.8 (74.4–92.3)	81.1 (68.4–88.9)	78.6 (68.2–86.0)	0.79†
BMI* (kg/m^2)	29.4 (25.7–31.7)	30.1 (26.8–32.1)	29.4 (25.1–31.3)	28.8 (24.6–31.5)	0.75†
Hypertension, n (%)	41 (50.0%)	17 (65.4%)	16 (44.4%)	8 (40.0%)	0.17‡
Dyslipidemia, n (%)	57 (69.5%)	24 (92.3)	19 (52.8%)	14 (70.0%)	<0.01‡
Smoking, n (%)	36 (43.9%)	11 (42.3%)	16 (44.4%)	9 (45.0%)	0.97‡
Sulfonylurea agent, n (%)	40 (48.8%)	18 (69.2%)	15 (41.7%)	7 (35.0%)	0.04‡
Metformin agent, n (%)	14 (17.1%)	0 (0%)	11 (30.6%)	3 (15.0%)	<0.01‡
AST* (IU/mL)	52 (35–61)	50 (32–59)	47 (36–56)	62 (40–85)	0.04†
ALT* (IU/mL)	75 (55–92)	65 (52–74)	75 (55–89)	87 (60–112)	0.07†
γ-GTP* (IU/mL)	93 (49–120)	98 (55–127)	89 (47–116)	95 (54–114)	0.85†
Fast blood glucose* (mg/dL)	187 (139–229)	207 (151–256)	175 (138–201)	182 (135–224)	0.10†
HbA1c (%)	8.2 (7.2–9.3)	8.4 (7.4–9.4)	8.4 (7.5–9.5)	7.7 (6.9–8.5)	0.22†
LDL-cholesterol* (mg/dL)	115 (95–140)	103 (78–116)	126 (104–148)	114 (92–140)	0.02†
Triglyceride* (mg/dL)	191 (117–240)	199 (125–283)	175 (114–229)	210 (130–198)	0.59†
Platelet count* ($\times 10^3/\mu$L)	206 (167–240)	204 (183–230)	216 (166 –248)	192 (147–233)	0.38†
APRI index*	0.75 (0.40–0.95)	0.73 (0.37–0.91)	0.64 (0.44–0.76)	0.96 (0.60–1.09)	0.04†

*Expressed as median (25th–75th percentiles).
†ANOVA.
‡Chi-square tests.
BMI: body mass index; AST: aspartate aminotransferase; ALT: alanine aminotransferase; γ-GTP: γ-glutamyl transpeptidase; HbA1c: hemoglobin A1c; APRI: AST-to-platelet counts ratio index.

finally up to the limit dose 0.9 mg if necessary. Sitagliptin was administered via oral route once daily 50 mg up to 100 mg if necessary. Pioglitazone was administered once daily 15 mg via oral route.

The beginning of followup was defined as the administration date of each medicine, and the end of follow-up was September 30, 2011. The followup consisted of monthly or bimonthly physical examination including body weight measurement and blood tests. Patients who completely changed each medicine to intensive therapies such as insulin injection because of exacerbation of diabetes were treated as end of follow at the moment of treatment change. Even if other oral glucose-lowering agents were added, the followup was considered to be valid as long as each medicine had still been continued. Patients who quitted each treatment due to improvement of diabetes were also treated as end of follow at the moment. The final decision of exacerbation or improvement of diabetes was made by our out patient clinic doctors' own assessments.

2.3. Statistical Analyses. Data were expressed as the median and range (25th–75th percentiles) unless otherwise indicated. Continuous variables among the three groups were compared by analysis of variance (ANOVA). Categorical variables were compared by chi-square test. Changes of parameters after the administration of each medicine were compared by paired t-test. There was no missing data. As previously mentioned, body weight reduction is an important treatment method for NAFLD patients [8]. Thus, we also tested the following variables obtained at the time of entry in univariate and multivariate logistic regression analysis to evaluate the factors which contribute to body weight reduction for over 5%; age, sex, BMI, presence of hypertension, existence of dyslipidemia, history of smoking, combination use of metformin or sulfonylurea agents, AST, ALT, γ-glutamyl transpeptidase (γ-GTP), fast blood sugar level, HbA1c, LDL-cholesterol, triglyceride, platelet counts, APRI index, and treatment modalities (liraglutide, sitagliptin, or pioglitazone). Parameters which P values were less than 0.10 included in the multivariate analysis. Nominal categorical data were represented by corresponding binary dummy variables. Data processing and analysis were performed using the StatView version 5.0 (SAS Institute Inc.).

3. Results

3.1. Patient Profile. The patients were divided into three groups according to the treatment modalities: liraglutide-treated group ($N = 26$), sitagliptin-treated group ($N = 36$), and pioglitazone-treated group ($N = 20$) (Figure 1). Baseline characteristics of each group were shown in Table 1. Dosing period of each drudges significantly different among the three groups ($P < 0.01$). The longest treatment period

Table 2: Change of parameters after administration of liraglutide.

Variables (N)	Liraglutide group ($N = 26$)		
	Before administration	After administration	Paired t-test P value
Body weight* (kg)	81.8 (74.4–92.3)	78.0 (72.1–88.5)	<0.01
BMI* (kg/m^2)	30.1 (26.8–32.1)	28.6 (25.5–31.6)	<0.01
AST* (IU/mL)	50 (32–59)	35 (29–39)	<0.01
ALT* (IU/mL)	65 (52–74)	48 (34–61)	<0.01
γ-GTP* (IU/mL)	98 (55–127)	90 (48–130)	0.44
Fast blood glucose* (mg/dL)	207 (151–256)	168 (116–199)	0.02
HbA1c (%)	8.4 (7.4–9.4)	7.6 (6.9–8.4)	0.01
LDL-cholesterol* (mg/dL)	103 (78–116)	99 (78–115)	0.51
Triglyceride* (mg/dL)	199 (125–283)	175 (114–231)	0.19
Platelet count* ($\times 10^3/\mu$L)	204 (183–230)	207 (173–224)	0.67
APRI index*	0.73 (0.37–0.91)	0.49 (0.34–0.56)	<0.01

BMI: body mass index; AST: aspartate aminotransferase; ALT: alanine aminotransferase; γ-GTP: γ-glutamyl transpeptidase; HbA1c: hemoglobin A1c; APRI: AST-to-platelet counts ratio index.

was observed in pioglitazone group. There were significant differences about the comorbidity with dyslipidemia among the three groups ($P < 0.01$). Comorbidity with dyslipidemia was higher in liraglutide group (92.3%). The combination use of metformin or sulfonylurea agents was significantly different among the three groups ($P < 0.01$ and $P = 0.04$, resp.). The proportion of combination use with metformin agents was higher in sitagliptin group (30.6%), and the proportion of combination use with sulfonylurea agents was higher in liraglutide group (69.2%). There were also significant differences about AST level, LDL-cholesterol level, and APRI index among the three groups ($P = 0.04$, $P = 0.02$, and $P = 0.04$, resp.). Pioglitazone group had advanced liver inflammation and fibrosis. There were no significant differences about other baseline characteristics among the three groups: age, proportion of male patients, body weight, BMI, comorbidity with hypertension, proportion of smoking patients, ALT level, γ-GTP level, fast blood glucose level, HbA1c level, Triglyceride level, and platelet counts.

3.2. Changes of Parameters after the Administration of Each Treatment. Table 2 showed the change of each parameter after administration of liraglutide. There was significant decrement in body weight and BMI; body weight decreased from 81.8 kg to 78.0 kg, and BMI decreased and from 30.1 kg/m^2 to 28.6 kg/m^2 (both $P < 0.01$). The control of diabetes mellitus also markedly improved: fast blood glucose decreased from 207 mg/dL to 168 mg/dL ($P = 0.02$) and HbA1c decreased from 8.4% to 7.6% ($P = 0.01$). Additionally, there was significant improvement of liver inflammation and liver fibrosis score; AST decreased from 50 IU/L to 35 IU/L, ALT decreased from 65 IU/L to 48 IU/L, and APRI index decreased from 0.73 to 0.49 (all $P < 0.01$).

Table 3 showed the change of each parameter after administration of sitagliptin. The control of diabetes mellitus significantly improved: fast blood glucose decreased from 175 mg/dL to 152 mg/dL and HbA1c decreased from 8.4% to 7.3% (both $P = 0.01$). LDL-cholesterol also markedly decreased from 126 mg/dL to 113 mg/dL ($P = 0.02$). Additionally, there was significant improvement of liver inflammation; ALT decreased from 75 IU/L to 61 IU/L ($P = 0.03$), and γ-GTP decreased from 89 IU/L to 75 IU/L ($P = 0.01$). However, body weight, BMI, AST level, and APRI index changes did not retain statistical significance.

Table 4 showed the change of each parameter after administration of pioglitazone. The control of diabetes mellitus significantly improved: fast blood glucose decreased from 182 mg/dL to 141 mg/dL, and HbA1c decreased from 7.7% to 6.9% (both $P = 0.01$). Triglyceride also markedly decreased from 210 mg/dL to 161 mg/dL ($P = 0.03$). Additionally, there was significant improvement of liver inflammation and liver fibrosis score; AST decreased from 62 IU/L to 41 IU/L, ALT decreased from 87 IU/L to 53 IU/L, γ-GTP decreased from 95 IU/L to 65 IU/L, and APRI index decreased from 0.96 to 0.73 (all $P < 0.01$). However, there was significant increment in body weight and BMI; body weight increased from 78.6 kg to 81.8 kg ($P < 0.01$), and BMI increased 28.8 kg/m^2 to 30.0 kg/m^2 ($P = 0.02$).

3.3. Logistic Regression Analysis about 5% Body Weight Reduction. As previously mentioned, body weight reduction for more than 5% is one of the important treatment of NAFLD [8]. Thus, we performed univariate and multivariate logistic regression analysis to clarify the parameters which affect on body weight reduction for over 5% (Table 5). In the univariate logistic regression analysis, administration of liraglutide, higher fast blood glucose level, and higher APRI index score were identified as significant factors contributing to body weight reduction ($P < 0.01$, $P < 0.01$, and $P = 0.04$, resp.). Combination use of sulfonylurea agents and higher AST level had also tendency to be significant factors affecting on body weight loss ($P = 0.07$ and $P = 0.09$, resp.). On the other hand, administration of sitagliptin was identified as a significant adverse factor on body weight reduction ($P < 0.01$). Higher serum albumin level also tended to be an adverse factor on body weight loss ($P = 0.06$). Adjusting

Table 3: Change of parameters after administration of sitagliptin.

Variables (N)	Sitagliptin ($N = 36$)		
	Before administration	After administration	Paired t-test P value
Body weight* (kg)	81.1 (68.4–88.9)	80.7 (68.7–86.3)	0.39
BMI* (kg/m^2)	29.4 (25.0–31.3)	29.2 (25.5–31.2)	0.56
AST* (IU/mL)	47 (36–56)	44 (30–45)	0.47
ALT* (IU/mL)	75 (55–89)	61 (40–74)	0.03
γ-GTP* (IU/mL)	89 (47–116)	75 (43–100)	0.01
Fast blood glucose* (mg/dL)	175 (138–201)	152 (128–187)	<0.01
HbA1c (%)	8.4 (7.5–9.5)	7.3 (6.5–7.8)	<0.01
LDL-cholesterol* (mg/dL)	126 (104–148)	113 (97–129)	0.02
Triglyceride* (mg/dL)	175 (114–229)	166 (99–195)	0.60
Platelet count* ($\times 10^3/\mu$L)	216 (166–248)	202 (162–240)	<0.01
APRI index*	0.64 (0.44–0.76)	0.60 (0.39–0.63)	0.47

BMI: body mass index; AST: aspartate aminotransferase; ALT: alanine aminotransferase; γ-GTP: γ-glutamyl transpeptidase; HbA1c: hemoglobin A1c; APRI: AST-to-platelet counts ratio index.

Table 4: Change of parameters after administration of pioglitazone.

Variables (N)	Pioglitazone group ($N = 20$)		
	Before administration	After administration	Paired t-test P value
Body weight* (kg)	78.6 (68.2–86.0)	81.8 (73.0–86.8)	<0.01
BMI* (kg/m^2)	28.8 (24.6–31.5)	30.0 (26.2–33.9)	0.02
AST* (IU/mL)	62 (40–85)	41 (26–47)	<0.01
ALT* (IU/mL)	87 (60–112)	53 (33–69)	<0.01
γ-GTP* (IU/mL)	95 (54–114)	65 (31–87)	<0.01
Fast blood glucose* (mg/dL)	182 (135–224)	141 (114–161)	<0.01
HbA1c (%)	7.7 (6.9–8.5)	6.9 (6.2–7.3)	<0.01
LDL-cholesterol* (mg/dL)	114 (92–140)	114 (87–140)	0.78
Triglyceride* (mg/dL)	210 (130–198)	161 (95–165)	0.03
Platelet count* ($\times 10^3/\mu$L)	193 (147–233)	184 (138–226)	0.14
APRI index*	0.96 (0.60–1.09)	0.73 (0.41–0.71)	0.01

BMI: body mass index; AST: aspartate aminotransferase; ALT: alanine aminotransferase; γ-GTP: γ-glutamyl transpeptidase; HbA1c: hemoglobin A1c; APRI: AST-to-platelet counts ratio index.

for these factors, multivariate logistic regression analysis indicated that administration of liraglutide and higher fast blood glucose level as independent factors affecting on body weight reduction for over 5% (both $P = 0.04$).

4. Discussion

NAFLD is a liver disease that is characterized histologically by hepatic steatosis, lobular inflammation, and hepatocellular ballooning [24], and it was reported that at least 3% of the patients progressed to cirrhosis [3]. The disorder is thought to be common because the incidence of its typical features, fatty liver disease, obesity, and type 2 DM, is increasing [25]. Multiple pharmacologic interventions have been attempted with variable success. Particularly, trials of glucose lowering agents such as metformin and pioglitazone have yielded promising results [18, 26]. In this study, drastic improvement of serum AST and ALT level was shown not only in pioglitazone group but also in liraglutide group and sitagliptin group, suggesting that treatment of diabetes improved insulin resistance and led to amelioration of liver inflammation in NAFLD patients with type 2 DM.

However, the improvement of liver inflammation and liver fibrosis is different matter. Since in a randomized controlled trial intended for NAFLD patients, pioglitazone demonstrated alteration of liver inflammation but did not affect on improvement of liver fibrosis [6]. Since this current study was based on outpatient clinic medial care, liver biopsy was not applied in our study population. Noninvasive measurement methods of liver stiffness, such as transient elastography, were not available in our institute. Thus, we applied APRI index to evaluate the degree of liver fibrosis [22]. In this current study, APRI index significantly improved between liraglutide group and pioglitazone group but not in sitagliptin group. The calculation of APRI index depended on changes in AST level and it might be one of the limitations

Table 5: Univariate and multivariate logistic regression analysis to evaluate the factors which contribute to body weight reduction for over 5%.

Variables	Odds ratio (95% CI) univariate	P	Odds ratio (95% CI) multivariate	P
Age (per year)	1.02 (0.97–1.07)	0.54		
Male	1.32 (0.33–5.28)	0.69		
Body weight (per 1.0 kg)	1.01 (0.98–1.05)	0.49		
BMI (per 1.0 kg/m^2)	1.06 (0.96–1.17)	0.23		
Hypertension	1.41 (0.44–4.51)	0.56		
Dyslipidemia	1.12 (0.31–3.97)	0.86		
Smoking	1.91 (0.59–6.10)	0.28		
Liraglutide	8.13 (2.24–29.5)	<0.01	9.04 (1.12–73.1)	0.04
Sitagliptin	0.17 (0.03–0.80)	<0.01	1.19 (0.12–12.0)	0.88
Pioglitazone	0.46 (0.09–2.27)	0.34		
Metformin	2.66 (0.08–9.30)	0.96		
Sulfonylurea	3.17 (0.90–11.1)	0.07	1.61 (0.28–9.43)	0.60
Albumin (per 1.0 mg/dL)	0.13 (0.01–1.13)	0.06	0.11 (0.01–2.42)	0.16
AST (per 10 IU/L)	1.22 (0.97–1.61)	0.09	1.03 (0.95–1.11)	0.47
ALT (per 10 IU/L)	1.05 (0.88–1.25)	0.54		
γ-GTP (per 10 IU/L)	1.05 (0.94–1.15)	0.33		
Fast blood glucose (per 10 mg/dL)	1.13 (1.03–1.26)	<0.01	1.14 (1.01–1.28)	0.04
HbA1c (per 1.0%)	1.32 (0.85–2.02)	0.21		
LDL-cholesterol (per 10 mg/dL)	0.87 (0.71–1.06)	0.16		
Triglyceride (per 10 mg/dL)	1.02 (0.98–1.06)	0.41		
Platelet counts (per $\times 10^4/\mu$L)	0.91 (0.82–1.02)	0.09	0.98 (0.72–1.33)	0.42
APRI index (per 1.0)	3.22 (0.01–997)	0.04	2.11 (0.01–332)	0.77

CI: confidence interval; BMI: body mass index; AST: aspartate aminotransferase; ALT: alanine aminotransferase; γ-GTP: γ-glutamyl transpeptidase; HbA1c: hemoglobin A1c; APRI: AST-to-platelet counts ratio index.

of this study. Nonetheless, the alteration of APRI index might be expected in these two groups. On the other hand, sitagliptin group had already lower serum AST level at the time of administration. It might be the main cause of no change in the APRI index at the end of followup. Although we could not clarify the true outcome of liraglutide on liver fibrosis, it was reported that GLP-1 analogue directly inhibited fibroblast growth factor 21 which promoted the progression of liver fibrosis in mice model [15]. Further more studies are needed.

Obesity is considered one of the most important risk factors for NAFLD [27]. Weight reduction via lifestyle intervention is generally recommended as an initial step in the management of NAFLD [27], and its effectiveness was proven in a randomized controlled trial [8]. However, lifestyle intervention depends on patient's own efforts and sometimes difficult to achieve the aim [28]. In this current study, the body weight dramatically changed after the administration of each treatment. Significant body weight reduction was shown in liraglutide group, significant body weight gain was shown in pioglitazone group, and body weight did not change in sitagliptin group. These results were supported by previous reports [13]. Besides, multivariate logistic regression analysis indicated that administration of liraglutide as an independent factor for body weight reduction. Although the first step in the management of NAFLD is lifestyle intervention, liraglutide may support body weight reduction via suppressing appetite and finally affect on improvement of NAFLD.

Since this current study based on a retrospective cohort, there were lots of limitations. The first limitation is that the difference of dosing period of each medicine. The median dosing period of pioglitazone was about 1200 days. On the other hand, the median dosing period of liraglutide and sitagliptin was about 340 days and 250 days, respectively. There was approximately fourfold difference, and the long-term outcome of liraglutide and sitagliptin was still unknown. The second limitation is that liraglutide is administered by subcutaneous injection. Sitagliptin and pioglitazone are oral drugs and considered to be less invasive than liraglutide. Continuing subcutaneous injection every day may be a great stress for patients even if weekly subcutaneous injective GLP-1 analogue (exenatide long-acting release) will be available in the near future. The last limitation is that this study cohort was consisted in patients treated with combination use of metformin agent. Metformin agent was reported to have some effects on liver steatosis and inflammation [26].

In conclusion, we have demonstrated the improvement of liver inflammation and diabetes in NAFLD patients with

type 2 DM treated by liraglutide, sitagliptin, and pioglitazone. However, APRI index did not alter in sitagliptin group, and body weight significantly increased in pioglitazone group. Aggravation of liver fibrosis score might lead future liver cirrhosis, and body weight gain could exacerbate liver inflammation and other metabolic disorders. Administration of liraglutide led not only to good control of type 2 DM but also improvement of liver inflammation, alteration of liver fibrosis, and reduction of body weight. Particularly, body weight reduction was a favorable outcome of applying liraglutide in NAFLD patients with type 2 DM.

Abbreviations

GLP-1: Glucagon like peptide-1
NAFLD: Nonalcoholic steatohepatitis
DM: Diabetes mellitus
DPP-4I: Dipeptidyl peptidase-4 inhibitor
DPP-4: Dipeptidyl peptidase-4
TZD: Thiazolidinedione
NASH: Nonalcoholic steatohepatitis
AST: Aspartate aminotransferase
ALT: Alanine aminotransferase
APRI: AST to platelet counts ratio index
HbA1c: Hemoglobin A1c
PPARγ: Peroxisome proliferator-activated receptor γ
BMI: Body mass index
ANOVA: Analysis of variance
γ-GTP: γ-glutamyl transpeptidase.

Conflict of Interests

The Authors declare that they have no conflict of interests.

Authors' Contribution

First author collected all data and wrote this paper. A. Isogawa, M. Iwamoto, M. Ohsugi, M. Toda, and K. Tagawa are outpatient clinic doctors who contributed to this study. H. Yoshida, M. Omata, and K. Koike checked up this paper and H. Yoshida is also the final corresponding author.

References

[1] J. M. Clark, F. L. Brancati, and A. M. Diehl, "The prevalence and etiology of elevated aminotransferase levels in the United States," *American Journal of Gastroenterology*, vol. 98, no. 5, pp. 960–967, 2003.

[2] M. Charlton, "Nonalcoholic fatty liver disease: a review of current understanding and future impact," *Clinical Gastroenterology and Hepatology*, vol. 2, no. 12, pp. 1048–1058, 2004.

[3] B. A. Neuschwander-Tetri and S. H. Caldwell, "Nonalcoholic steatohepatitis: summary of an AASLD single topic conference," *Hepatology*, vol. 37, no. 5, pp. 1202–1219, 2003.

[4] F. Angelico, M. Del Ben, R. Conti et al., "Insulin resistance, the metabolic syndrome, and nonalcoholic fatty liver disease," *Journal of Clinical Endocrinology and Metabolism*, vol. 90, no. 3, pp. 1578–1582, 2005.

[5] C. P. Day and O. F. W. James, "Steatohepatitis: a tale of two "Hits"?" *Gastroenterology*, vol. 114, no. 4, pp. 842–845, 1998.

[6] A. J. Sanyal, N. Chalasani, K. V. Kowdley et al., "Pioglitazone, vitamin E, or placebo for nonalcoholic steatohepatitis," *The New England Journal of Medicine*, vol. 362, no. 18, pp. 1675–1685, 2010.

[7] J. B. Dixon, P. S. Bhathal, N. R. Hughes, and P. E. O'Brien, "Nonalcoholic fatty liver disease: improvement in liver histological analysis with weight loss," *Hepatology*, vol. 39, no. 6, pp. 1647–1654, 2004.

[8] K. Promrat, D. E. Kleiner, H. M. Niemeier et al., "Randomized controlled trial testing the effects of weight loss on nonalcoholic steatohepatitis," *Hepatology*, vol. 51, no. 1, pp. 121–129, 2010.

[9] D. J. Drucker and M. A. Nauck, "The incretin system: glucagon-like peptide-1 receptor agonists and dipeptidyl peptidase-4 inhibitors in type 2 diabetes," *The Lancet*, vol. 368, no. 9548, pp. 1696–1705, 2006.

[10] C. Verdich, A. Flint, J. P. Gutzwiller et al., "A meta-analysis of the effect of glucagon-like peptide-1 (7-36) amide on Ad Libitum energy intake in humans," *Journal of Clinical Endocrinology and Metabolism*, vol. 86, no. 9, pp. 4382–4389, 2001.

[11] M. Zander, S. Madsbad, J. L. Madsen, and J. J. Holst, "Effect of 6-week course of glucagon-like peptide 1 on glycaemic control, insulin sensitivity, and β-cell function in type 2 diabetes: a parallel-group study," *The Lancet*, vol. 359, no. 9309, pp. 824–830, 2002.

[12] H. Agersø, L. B. Jensen, B. Elbrønd, P. Rolan, and M. Zdravkovic, "The pharmacokinetics, pharmacodynamics, safety and tolerability of NN2211, a new long-acting GLP-1 derivative, in healthy men," *Diabetologia*, vol. 45, no. 2, pp. 195–202, 2002.

[13] M. Marre, J. Shaw, M. Brändle et al., "Liraglutide, a once-daily human GLP-1 analogue, added to a sulphonylurea over 26 weeks produces greater improvements in glycaemic and weight control compared with adding rosiglitazone or placebo in subjects with Type 2 diabetes (LEAD-1 SU)," *Diabetic Medicine*, vol. 26, no. 3, pp. 268–278, 2009.

[14] N. A. Gupta, J. Mells, R. M. Dunham et al., "Glucagon-like peptide-1 receptor is present on human hepatocytes and has a direct role in decreasing hepatic steatosis *in vitro* by modulating elements of the insulin signaling pathway," *Hepatology*, vol. 51, no. 5, pp. 1584–1592, 2010.

[15] S. L. Samson, P. Sathyanarayana, M. Jogi et al., "Exenatide decreases hepatic fibroblast growth factor 21 resistance in non-alcoholic fatty liver disease in a mouse model of obesity and in a randomised controlled trial," *Diabetologia*, vol. 54, no. 12, pp. 3093–3100, 2011.

[16] C. H. S. McIntosh, H. U. Demuth, J. A. Pospisilik, and R. Pederson, "Dipeptidyl peptidase IV inhibitors: how do they work as new antidiabetic agents?" *Regulatory Peptides*, vol. 128, no. 2, pp. 159–165, 2005.

[17] G. Firneisz, T. Varga, G. Lengyel et al., "Serum dipeptidyl peptidase-4 activity in insulin resistant patients with non-alcoholic fatty liver disease: a novel liver disease biomarker," *PLoS ONE*, vol. 5, no. 8, Article ID e12226, 2010.

[18] R. Belfort, S. A. Harrison, K. Brown et al., "A placebo-controlled trial of pioglitazone in subjects with nonalcoholic steatohepatitis," *The New England Journal of Medicine*, vol. 355, no. 22, pp. 2297–2307, 2006.

[19] Y. Miyazaki, A. Mahankali, M. Matsuda et al., "Effect of pioglitazone on abdominal fat distribution and insulin sensitivity in type 2 diabetic patients," *Journal of Clinical Endocrinology and Metabolism*, vol. 87, no. 6, pp. 2784–2791, 2002.

[20] B. A. Neuschwander-Tetri, E. M. Brunt, K. R. Wehmeier, D. Oliver, and B. R. Bacon, "Improved nonalcoholic steatohepatitis after 48 weeks of treatment with the PPAR-γ ligand rosiglitazone," *Hepatology*, vol. 38, no. 4, pp. 1008–1017, 2003.

[21] B. Balas, R. Belfort, S. A. Harrison et al., "Pioglitazone treatment increases whole body fat but not total body water in patients with non-alcoholic steatohepatitis," *Journal of Hepatology*, vol. 47, no. 4, pp. 565–570, 2007.

[22] C. T. Wai, J. K. Greenson, R. J. Fontana et al., "A simple noninvasive index can predict both significant fibrosis and cirrhosis in patients with chronic hepatitis C," *Hepatology*, vol. 38, no. 2, pp. 518–526, 2003.

[23] E. von Elm, M. Egger, D. G. Altman, S. J. Pocock, P. C. Gøtzsche, and J. P. Vandenbroucke, "Strengthening the reporting of observational studies in epidemiology (STROBE) statement: guidelines for reporting observational studies," *British Medical Journal*, vol. 335, no. 7624, pp. 806–808, 2007.

[24] J. Ludwig, T. R. Viggiano, D. B. McGill, and B. J. Ott, "Nonalcoholic steatohepatitis. Mayo Clinic experiences with a hitherto unnamed disease," *Mayo Clinic Proceedings*, vol. 55, no. 7, pp. 434–438, 1980.

[25] J. D. Browning, L. S. Szczepaniak, R. Dobbins et al., "Prevalence of hepatic steatosis in an urban population in the United States: impact of ethnicity," *Hepatology*, vol. 40, no. 6, pp. 1387–1395, 2004.

[26] E. Bugianesi, E. Gentilcore, R. Manini et al., "A randomized controlled trial of metformin versus vitamin E or prescriptive diet in nonalcoholic fatty liver disease," *American Journal of Gastroenterology*, vol. 100, no. 5, pp. 1082–1090, 2005.

[27] G. Marchesini, M. Brizi, G. Blanchi et al., "Nonalcoholic fatty liver disease: a feature of the metabolic syndrome," *Diabetes*, vol. 50, no. 8, pp. 1844–1850, 2001.

[28] R. T. Wang, R. L. Koretz, and H. F. Yee, "Is weight reduction an effective therapy for nonalcoholic fatty liver? A systematic review," *American Journal of Medicine*, vol. 115, no. 7, pp. 554–559, 2003.

Modulation of lipid metabolism with the overexpression of NPC1L1 in mouse liver[S]

Makoto Kurano,*,† Masumi Hara,§ Koichi Tsuneyama, Koji Okamoto,†† Naoyuki Iso-O,§§ Teruhiko Matsushima,*** Kazuhiko Koike,††† and Kazuhisa Tsukamoto[1],*,§§§**

Departments of Metabolic Diseases,* Clinical Laboratory Medicine,† Nephrology and Endocrinology,†† and Gastroenterology,††† Graduate School of Medicine, University of Tokyo, Japan; The Forth Department of Internal Medicine,§ Teikyo University Mizonokuchi Hospital, Kawasaki, Japan; Department of Diagnostic Pathology,** Graduate School of Medicine and Pharmaceutical Sciences, University of Toyama, Toyama, Japan; Department of Advanced Medical Science,§§ The Institute of Medical Science, University of Tokyo, Tokyo, Japan; Department of Food and Health Science,*** Faculty of Human Life Science, Jissen Women's University, Hino, Japan; and Department of Metabolism, Diabetes and Nephrology,§§§ Preparatory Office for Aizu Medical Center, Fukushima Medical University, Fukushima, Japan

Abstract Niemann-Pick C1-like 1 protein (NPC1L1), a transporter crucial in intestinal cholesterol absorption, is expressed in human liver but not in murine liver. To elucidate the role of hepatic NPC1L1 on lipid metabolism, we overexpressed NPC1L1 in murine liver utilizing adenovirus-mediated gene transfer. C57BL/6 mice, fed on normal chow with or without ezetimibe, were injected with NPC1L1 adenovirus (L1-mice) or control virus (Null-mice), and lipid analyses were performed five days after the injection. The plasma cholesterol levels increased in L1-mice, and FPLC analyses revealed increased cholesterol contents in large HDL lipoprotein fractions. These fractions, which showed α-mobility on agarose electrophoresis, were rich in apoE and free cholesterol. These lipoprotein changes were partially inhibited by ezetimibe treatment and were not observed in apoE-deficient mice. In addition, plasma and VLDL triglyceride (TG) levels decreased in L1-mice. The expression of microsomal triglyceride transfer protein (MTP) was markedly decreased in L1-mice, accompanied by the reduced protein levels of forkhead box protein O1 (FoxO1). These changes were not observed in mice with increased hepatic de novo cholesterol synthesis. These data demonstrate that cholesterol absorbed through NPC1L1 plays a distinct role in cellular and plasma lipid metabolism, such as the appearance of apoE-rich lipoproteins and the diminished VLDL-TG secretion.—Kurano, M., M. Hara, K. Tsuneyama, K. Okamoto, N. Iso-O, T. Matsushima, K. Koike, and K. Tsukamoto. **Modulation of lipid metabolism with the overexpression of NPC1L1 in mouse liver.** ***J. Lipid Res.*** **2012.** 53: **2275–2285.**

Supplementary key words biliary cholesterol • apoE-rich lipoprotein • ezetimibe • Niemann-Pick C1-like 1 protein

Dyslipidemia has proved to be a major risk factor for cardiovascular diseases, and many lipid-lowering agents have been demonstrated to reduce the incidence of cardiovascular diseases. Ezetimibe is a recent lipid-lowering agent known to inhibit cholesterol absorption from the intestine (1). The main clinical benefit of ezetimibe is to lower LDL cholesterol levels (2–5); however, there have been reports of other beneficial effects of ezetimibe, such as lowering plasma triglycerides levels (3, 5, 6).

Niemann-pick C1-like 1 protein (NPC1L1) (7, 8), a target protein of ezetimibe, exists in the plasma membrane and early endosome and plays a key role in the intestinal absorption of free cholesterol (9–11). The cholesterol entering the plasma membrane is detected by NPC1L1 and internalized in the endocytic recycling compartment. Interestingly, the difference in the expression levels of NPC1L1 among various tissues differ among species; in humans, the level of NPC1L1 expression in the liver is almost the same as that of the intestine; however, there is little hepatic NPC1L1 expression in rodents, especially in mice (7). Previous work by Temel et al., which utilized transgenic mice stably expressing NPC1L1 in the liver, demonstrated that hepatic NPC1L1 played a critical role in the absorption of cholesterol from the bile (12). This observation enriched our knowledge regarding the sources of cholesterol in the human liver; besides the de novo synthesis

Abbreviations: CETP, cholesteryl ester transfer protein; ER, endoreticulum; ERL, apoE-rich lipoprotein; EZ, ezetimibe; FoxO1, forkhead box protein O1; FPLC, fast protein liquid chromatography; LSS, lanosterol synthase; MTP, microsomal triglyceride transfer protein; NPC1L1, Niemann-Pick C1-like 1 protein; SR-BI, scavenger receptor class B, type I; TG, triglyceride; GPT, glutamic pyruvic transaminase.

[1] To whom correspondence should be addressed.
e-mail: kazut@fmu.ac.jp

[S] The online version of this article (available at http://www.jlr.org) contains supplementary data in the form of 11 figures.

This research was supported by Grants-in-Aid 20591079 (K. Tsukamoto) and 23591330 (K. Tsukamoto) from the Japan Society for the Promotion of Science.

Manuscript received 17 March 2012 and in revised form 11 August 2012.

Published, JLR Papers in Press, August 13, 2012
DOI 10.1194/jlr.M026575

of cholesterol and cholesterol supply from the sinusoidal side of the cells through lipoproteins, human hepatocytes acquire cholesterol from the bile duct canaliculi as well.

Several lines of evidence have shown that hepatic cholesterol derived from different sources has undergone different metabolic pathways; for example, cholesterol taken up through scavenger receptor class B, type I (SR-BI) from HDL particles is believed to be preferentially secreted in the bile (13, 14), whereas cholesterol newly synthesized or acquired via LDL receptors is secreted into the blood circulation or stored in the cells. Thus, it is plausible to hypothesize that cholesterol acquired through NPC1L1 from the canalicular side of the hepatocytes undergoes a different pathway from that of other origins and may possess novel metabolic properties on lipid and lipoprotein metabolism.

In this study, we examined the influence of hepatic NPC1L1 expression on lipoprotein metabolism utilizing adenovirus-mediated gene transfer. Stable inbred expression of a target protein utilizing transgenic animals would result in the secondary metabolic changes to maintain homeostasis and, in doing so, obscure the genuine metabolic effects of the target protein. On the other hand, abrupt and adventitious protein expression using an adenoviral-vector enabled us to examine the metabolic effect of the expressed protein with minimal secondary metabolic changes. Through this study, we found two interesting effects on lipoprotein metabolism with hepatic NPC1L1 expression; namely, we observed the emergence of apoE-rich lipoprotein (ERL) as well as a decrease in serum VLDL-triglyceride (TG). Besides this observation, we could clarify that cholesterol absorbed through NPC1L1 might possess physiological properties that are distinct from cholesterol derived from other origins.

EXPERIMENTAL PROCEDURES

Generation of recombinant adenoviruses

Human NPC1L1 and LSS cDNAs were cloned from the cDNA library of human liver (Takara Bio Inc., Shiga, Japan) and peripheral blood mononuclear cells, respectively. Human NPC1L1 adenovirus (Ad-L1) and human LSS adenovirus (Ad-LSS) were constructed with AdEasy system (Stratagene, La Jolla, CA) and purified through CsCl gradient centrifugation. Control adenovirus (Ad-Null), which lacks encoded cDNA, was also constructed.

For the in vivo analyses, adenoviral vectors were administered with a dose of 1×10^{11} particles (6.5×10^{9} pfu) via the tail vein into mice. For the in vitro experiments, the cells were infected with adenoviruses at the MOI of 25.

Cell samples

HepG2 cells, purchased from American Type Culture Collection (ATCC; Manassas, VA), were cultured in DMEM (Sigma-Aldrich Co.) supplemented with 10% fetal bovine serum (FBS; Gibco BRL, Eggstein, Germany) and 1% penicillin/streptomycin (Gibco BRL).

To analyze the effects of NPC1L1 expression in HepG2 cells, 2 days after the viral infection, the medium was replaced with serum-free, bile micelle-containing DMEM. Bile micelle was prepared as described previously (15); sodium taurocholate (Sigma-Aldrich Co.) dissolved in 96% ethanol, egg-yolk phosphatidylcholine (Sigma-Aldrich Co.) dissolved in methanol, and cholesterol (WAKO Pure Chemical Industries, Osaka, Japan) dissolved in ethanol were briefly mixed together, evaporated under nitrogen gas flow, stirred in DMEM for 6 h at 37°C, and filtered before use. The final concentrations of sodium taurocholate, egg-yolk phosphatidylcholine, and cholesterol were 2 mM, 40 μM, and 0.1 mM, respectively.

For the analysis of the effects of cellular de novo cholesterol synthesis on the FoxO1 protein level, the medium was replaced with serum-free DMEM containing 10 μM pitavastatin (Chemtech Labo., Inc., Tokyo, Japan) with or without 30 mM mevalonate (Sigma-Aldrich Co.). The cells were subjected to analyses 24 h after changing the medium.

Animal models

C57BL/6 mice and apoE-deficient mice were purchased from CLEA Japan (Tokyo, Japan) and Sankyo Lab Service Co. (Tokyo, Japan), respectively. Ezetimibe-containing chow (10 mg/100 g food) (16) was prepared by mixing Zetia tablets (Schering, Kenilworth, NJ) dissolved in carboxymethyl cellulose (Sigma-Aldrich Co.) with normal chow (Oriental Yeast Co, Tokyo, Japan). Six-week-old mice were fed with normal chow containing ezetimibe [EZ(+)] or vehicle [EZ(−)] for 3 weeks, after which they were injected with adenoviral vectors. Animal experiments were approved by the animal committee within the University of Tokyo.

Immunohistochemical analysis

Liver samples of mice infected with Ad-L1 or Ad-Null were fixed with 4% paraformaldehyde, sectioned into 5 μm thick slices, and processed for immunohistochemistry utilizing rabbit anti-NPC1L1 antibody (Cayman Chemical Co, Ann Arbor, MI) as a primary antibody and peroxidase-labeled polymer of goat anti-rabbit Ig antibody (Envision system, Dako, Glostrup, Denmark) as the secondary antibody. Color development was performed with DAB, and the samples were counterstained by hematoxylin.

Analyses of bile acid, phospholipids, and cholesterol contents of the bile

The bile was harvested from the gall bladders of anesthetized mice and mixed with methanol and chloroform. The aqueous phase was utilized to assess total bile acids using enzymatic methods (WAKO Pure Chemical Industries); the organic phase was designed to assess phospholipids through enzymatic methods (WAKO Pure Chemical Industries) and cholesterol using HPLC as described previously (17).

Analysis of plasma lipoprotein profiles

Five days after the injection of adenoviruses, the mice were fasted for 6 h, and blood samples were collected. Total and free cholesterol, triglycerides, and phospholipids were measured with enzymatic methods (WAKO Pure Chemical Industries). The values of esterified sterol were calculated by subtracting free sterol values from total sterol values and then multiplying by 1.67. The plasma samples were also subjected to Western blot analyses with anti-apoA-I antibody, anti-apoE antibody (Chemicon International Inc., Temecula, CA), and anti-apoB antibody (Calbiochem Inc., La Jolla, CA), after which plasma apolipoprotein levels were calculated with densitometric analyses of the blots.

Plasma samples were pooled and separated by FPLC utilizing Superose 6 column. The pooled plasma and several FPLC fractions were further separated by agarose electrophoresis with universal gel/8 (Helena Laboratory, Saitama, Japan). The agarose gels were stained with Fat Red 7B (Sigma-Aldrich Co.) to analyze the lipoprotein distribution; for the analyses, proteins on the gels were transferred to nitrocellulose membranes, followed by immunoblotting as described below.

Measurement of cellular and hepatic lipid contents

Cellular and hepatic lipid was extracted with methanol and chloroform, and the cholesterol and triglycerides levels were measured with enzymatic methods. The levels of cholesterol and triglycerides were adjusted with the cellular or hepatic protein levels.

Preparation and Western blot analyses of liver homogenates and cell lysates

For the preparation of whole cellular proteins, murine livers and HepG2 cells were homogenized in RIPA lysis buffer (Santa Cruz Biotechnology, Santa Cruz, CA). For the preparation of membranous protein, murine livers and HepG2 cells were homogenized in 5 mM Tris-HCl (pH 7.5) solution containing 1 mM PMSF and protease inhibitor cocktail (Roche, Mannheim, Germany) and centrifuged at 700 *g* for 15 min three times. The supernatants were centrifuged at 444,000 *g* for 60 min, and the pellets were suspended in 50 mM Tris-HCl (pH7.5) solution containing 1% TritonX-100, 5 mM EDTA, 10 mM EGTA, and 1 mM PMSF. The nuclear fractions were prepared as described previously (18).

Protein analyses with Western blot were performed using the following antibodies; anti-Erk and anti-phospho Erk antibody (BD Bioscience, San Jose, CA); anti-FoxO1 (Ser256) antibody (GenScript Co., Piskataway, NJ); anti-β-actin antibody (MBL, Nagoya, Japan); anti-NPC1L1 and anti-LDL receptor antibody (Cayman Chemical Co., Ann Arbor, MI); anti-ABCA1 antibody (Novus Biologicals, Inc., Littleton, CO); anti-pan cadherin antibody (Thermo Fisher Scientific Inc., Fremont, CA); and anti-SREBP-1, SREBP-2, and laminA/C antibody (Santa Cruz Biotechnology).

Real-time PCR

Total RNAs extracted from murine livers with GenElute mammalian total RNA miniprep kit (Sigma-Aldrich) were subjected to reverse transcription with Superscript II enzyme (Invitrogen Co.). Real-time quantitative PCR was performed with LightCycler system (Roche Diagnostics, Basel, Switzerland). Hybridization probes and primers were obtained from Nihon Gene Research Laboratories, Inc. (Sendai, Japan). The expression levels of the genes of interest were adjusted to those of the endogenous control GAPDH mRNA.

Hepatic VLDL-TG production assay

Five days after the adenovirus injection, mice were fasted for 5 h, and then injected with a 500 mg/kg body weight dose of tyloxapol (Sigma-Aldrich Co.) (19). Blood samples were collected at 0, 40, 80, and 120 min and measured for triglycerides.

Statistical analysis

The results were expressed as mean ± SEM. Differences between two groups were evaluated with Student *t*-test, and the differences among more than two groups were assessed using one-way ANOVA, followed by multiple comparison tests. *P*-values less than 0.05 were deemed as statistically significant.

RESULTS

Increased uptake of free cholesterol from bile micelles with the expression of NPC1L1 in HepG2 cells

To demonstrate that NPC1L1 expression with human NPC1L1 adenovirus (Ad-L1) increased the uptake of cholesterol in the bile micelle, HepG2 cells infected with Ad-L1 or control adenovirus (Ad-Null) were loaded with bile micelles, and the cellular cholesterol contents were evaluated. As shown in **Fig. 1**, cellular infection of Ad-L1 increased NPC1L1 protein contents (Fig. 1A) and resulted in a significant increase in cellular free cholesterol, which was inhibited by ezetimibe treatment (Fig. 1B). Incubation of the cells for a longer period resulted in a significant increase in cellular cholesteryl ester content as well, which would be a consequence of the esterification of free cholesterol (supplementary Fig. I). These results indicated that NPC1L1, expressed with Ad-L1, absorbed free cholesterol from the bile micelles.

Localization of overexpressed NPC1L1 protein in mice liver and its effect on biliary cholesterol concentration

We overexpressed NPC1L1 protein in C57BL/6 mice and evaluated its effect on the lipid contents in the bile. Western blot analysis of the liver samples confirmed that the administration of Ad-L1 into C57BL/6 mice resulted in the increase of NPC1L1 protein in the liver (Fig. 1C). Furthermore, immunohistochemical analysis of the liver specimens showed that the overexpressed NPC1L1 protein was mainly localized to the bile canalicular surface (Fig. 1D, E), which was concordant with the NPC1L1 localization in human liver.

Analysis of the lipid and bile acid contents of the bile showed a significant and drastic decrease in the biliary cholesterol levels with no changes in concentration of bile acids (Fig. 1F), indicating that overexpressed NPC1L1 protein localized to the canalicular side had absorbed cholesterol from the bile. Concordant with this observation, hepatic cholesterol contents increased almost in parallel with hepatic NPC1L1 expression (supplementary Fig. II). The biliary phospholipid concentrations also decreased by as much as 50% (Fig. 1F) with the overexpression of NPC1L1.

Modulation of plasma lipid profiles with the overexpression of NPC1L1 in C57BL/6 mice

We next analyzed the effects of hepatic NPC1L1 expression on plasma lipoprotein metabolism. As shown in **Fig. 2A**, hepatic NPC1L1 expression dramatically increased plasma total cholesterol levels (96 mg/dl versus 155 mg/dl, $P < 0.01$); this increase was partially inhibited by ezetimibe treatment [EZ(+)]. Plasma phospholipids were also increased by hepatic NPC1L1 expression (supplementary Fig. III-A). As for plasma apolipoprotein levels, hepatic NPC1L1 expression increased plasma apoE, apoB100, and apoB48; however, no difference was observed in plasma apoA-I (Fig. 2B, supplementary Fig. III-B, C).

To analyze more extensively the lipoprotein changes induced by NPC1L1 overexpression, pooled plasma samples were subjected to fast protein liquid chromatography (FPLC) analysis. As shown in Fig. 2C, the increase in plasma cholesterol levels found in mice administered Ad-L1 (L1-mice) was due to the increase in those of LDL fractions (fractions 30–34) and of fractions whose particle sizes ranged between those of LDL and HDL (fractions 36–40). The increase in cholesterol levels in these fractions was partially reversed by ezetimibe treatment; however, in

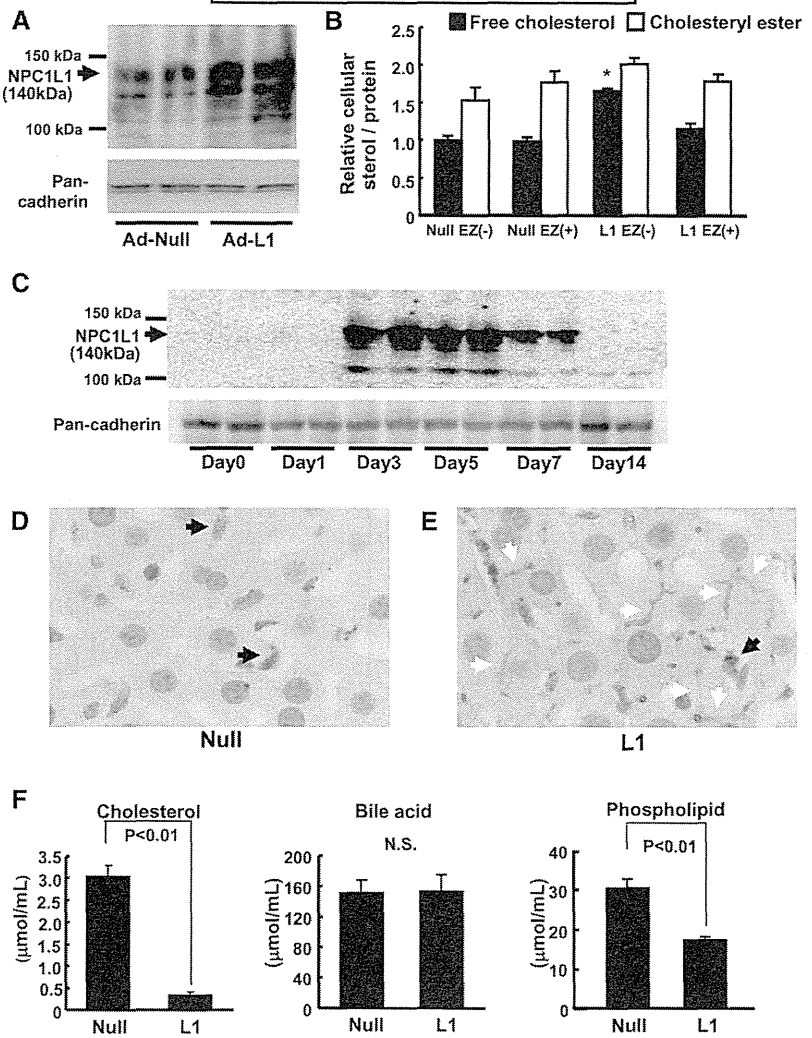

Fig. 1. Overexpression of NPC1L1 in murine liver facilitated the uptake of cholesterol from the bile. (A, B) HepG2 cells infected with Ad-L1 (L1) or Ad-Null (Null). (A) Western blot analysis of cellular membranous proteins for NPC1L1. (B) Cellular free cholesterol uptake from bile micelle (n = 3). $*P < 0.01$ compared with other groups. (C–F) C57BL/6 mice were administered Ad-L1 (L1) or Ad-Null (Null). (C) Time course changes of the hepatic NPC1L1 protein. Western blot analyses for NPC1L1 protein were performed with the cellular membranous proteins of the liver. (D, E) Immunohistochemical analysis of the liver for NPC1L1. (D) Null-mice and (E) L1-mice. White arrows indicate NPC1L1 protein along the bile canaliculi, and black arrows represent Kupffer cells. (F) Cholesterol, bile acid, and phospholipid levels in the bile obtained from gallbladder (n = 4).

mice injected with Ad-Null (Null-mice), treatment with ezetimibe did not affect the FPLC cholesterol profile, suggesting that the lipoprotein changes found in L1-mice emerged as a result of hepatic NPC1L1 expression. Changes in cholesterol levels were not observed in VLDL fractions (fractions 22–24) and HDL fractions (fractions 41–45). Analysis of free cholesterol levels among FPLC fractions revealed that fractions 36–40 of L1-mice were markedly rich in free cholesterol; specifically, about 50% of cholesterol was free cholesterol (supplementary Fig. III-D). The phospholipid contents of fractions 36–40 of L1-mice increased as well (supplementary Fig. III-E). Western blot analyses of FPLC fractions demonstrated that apoE protein levels increased markedly in fractions 36–40, indicating that these fractions were apoE-rich lipoproteins (ERL) (Fig. 2D). ApoE protein was also abundant in fractions 30–34, implying that fractions 30–34 were composed of not only LDL particles but also ERLs.

Previous studies have suggested that several classes of lipoproteins, such as pre-β1, pre-β2, or α-migrating lipoproteins (20, 21), possess the potency to represent ERL. Thus, to characterize the ERLs found in L1-mice, plasma and FPLC samples were subjected to agarose electrophoresis. Agarose electrophoresis of the plasma revealed that

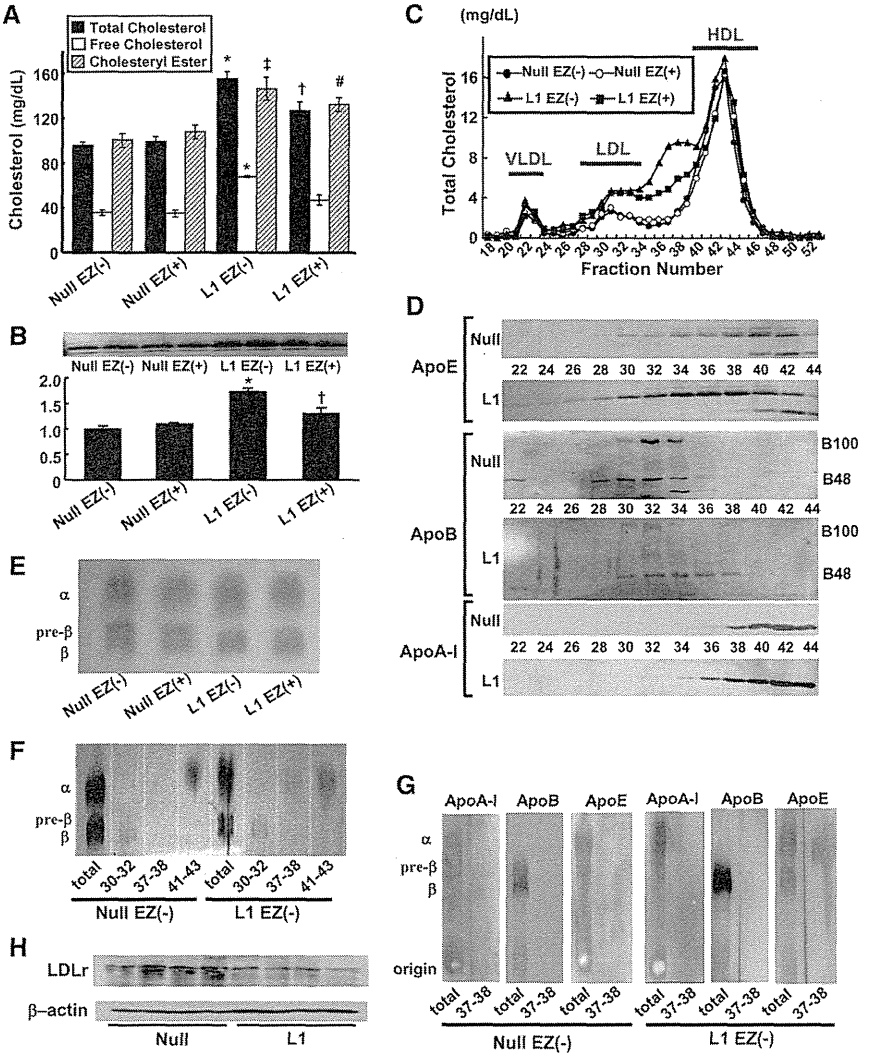

Fig. 2. Increased plasma cholesterol levels and the appearance of apoE-rich lipoproteins with the overexpression of NPC1L1 in murine liver. Six-week-old C57BL6 mice were fed with normal chow containing ezetimibe [EZ(+)] or vehicle [EZ(−)] for 3 weeks, and then they were administered Ad-L1 (L1) or Ad-Null (Null). Five days after the viral administration, plasma samples were collected after 6 h fasting (n = 3–5/each group). (A) Plasma total and free cholesterol levels were measured with enzymatic methods. $^{*}P < 0.01$ versus Null EZ(−) and Null EZ(+), and $P < 0.05$ versus L1 EZ(+); $^{\dagger}P < 0.05$ versus the other groups; $^{\ddagger}P < 0.01$ versus Null EZ(−), and $P < 0.05$ versus Null EZ(+); $^{\#}P < 0.05$ versus Null EZ(−). (B) Plasma apoE was determined with Western blot analysis. $^{*}P < 0.01$ compared with Null EZ(−), Null EZ(+), and $P < 0.05$ compared with L1 EZ(+); $^{\dagger}P < 0.01$ compared with Null EZ(−) and Null EZ(+). (C, D) Pooled plasma samples from each group were separated by FPLC, and fractions were subjected to cholesterol measurements and Western blot analyses. Panel C represents the total cholesterol profile, and panel D represents the results of Western blot analyses for apoE, apoB, and apoA-I proteins among the FPLC fractions. (E–G) Pooled plasma samples and FPLC-fractionated samples from Null EZ(−), Null EZ(+), L1 EZ(−), and L1 EZ(+) were subjected to agarose gel electrophoresis. The gels were either stained with Fat Red 7B (panels E, F) or blotted to nitrocellulose membranes followed by Western blot analyses (panel G). (E) Fat Red 7B staining of the gels electrophoresed with pooled plasma samples. (F) Pooled plasma samples (total) or some FPLC fractions (30–32, 37–38, and 41–43) were subjected to agarose gel electrophoresis, followed by Fat Red 7B staining. (G) Pooled plasma samples (total) or FPLC fractions (37–38) were subjected to agarose gel electrophoresis, followed by Western blot analyses for apoA-I, apoB and apoE. (H) Western blot analyses for hepatic LDL receptor protein. β-Actin was used as an internal control.

the lipid contents of pre-β lipoproteins were decreased in L1-mice (Fig. 2E), suggesting decreased neutral lipids in VLDL fractions. FPLC fractions 30–32 and fractions 41–43 showed β- and α-mobility on agarose electrophoresis, respectively, confirming that they were LDL and HDL fractions (Fig. 2F). Lipoproteins of fractions 37–38, which were abundant in apoE, showed α-mobility (Fig. 2F); furthermore, Western blot analysis of the agarose gel electrophoresed

with fractions 37–38 revealed the existence of apoE exclusively in the α-position, with no detection of apoA-I and apoB proteins (Fig. 2G). Thus, these results demonstrated that ERLs found in L1-mice were homogeneous and had α-mobility on agarose electrophoresis, which could be classified as large HDL particles.

Analyses of the ERL production mechanism

To elucidate the mechanism behind the appearance of ERL in L1-mice, we first examined whether Ad-L1 administration affected the intestinal sterol absorption. As shown in supplementary Fig. IV, absorption of sterol from intestine of L1-mice was almost the same as that of Null-mice, suggesting that the appearance of ERL was not due to the modulation in intestinal cholesterol absorption in L1-mice. Ezetimibe treatment in L1-mice understandably suppressed sterol absorption significantly (supplementary Fig. IV), which might be associated with the reduced plasma total cholesterol levels in EZ-treated L1-mice. Second, to clarify that ERLs were produced directly from hepatocytes, the media of HepG2 cells treated with Ad-L1 together with bile micelles were subjected to FPLC analyses. As shown in supplementary Fig. V, apoE protein in the media was distributed in fractions 36–40 as well as in other lipoprotein fractions, confirming that ERLs were directly produced from L1-expressing HepG2 cells. Furthermore, ezetimibe treatment efficiently suppressed apoE levels in fractions between LDL and HDL, suggesting that cholesterol absorbed through NPC1L1 would be secreted dominantly as ERL.

We next analyzed the factors believed to be relevant to ERL production in the liver. One of the candidates is the increased ATP binding cassette transporter A1 (ABCA1) protein levels, which has been proposed in two different lines of studies (12, 22); however, ABCA1 protein level was not altered in Ad-L1 mice (supplementary Fig. VI-A). Up-regulation of hepatic apoE, which has been shown to be associated with increased ERL production in HepG2 spheroids when treated with a LXR agonist (18), was the other candidate; however, hepatic apoE protein and mRNA levels were unaltered (supplementary Fig. VI-B, C). Thus, hepatic ABCA1 and apoE expression levels were not the key factors behind ERL production.

As shown in Fig. 2H, the protein levels of LDL receptor decreased in L1-mice, which would have led to an increase in plasma apoB100 levels due to the decreased clearance of LDL particles (supplementary Fig. III-C). Furthermore, the clearance of chylomicron remnants, analyzed by retinol palmitate test, was also retarded in L1-mice (supplementary Fig. VII), suggesting the reduced levels of remnant receptors. Thus, it is plausible that the clearance of ERLs might also be retarded due to the reduced levels of receptors associated with lipoprotein clearance, which might contribute to the appearance of ERLs.

Overexpression of NPC1L1 in ApoE-deficient mice

To investigate the role of apoE in the production of large HDL and elucidate the physiological effect of ERL, hepatic expression of NPC1L1 was performed in apoE-deficient mice. Overexpression of NPC1L1 in apoE-deficient mice resulted in a significant increase in plasma free cholesterol (**Fig. 3A**) and phospholipid levels (data not shown) as was observed in C57BL/6 mice. FPLC analysis of plasma samples, however, showed a distinct difference from that found in wild-type mice; large HDL particles, which corresponded to fractions 36–40, did not emerge in apoE-deficient mice (Fig. 3B, C), suggesting that the apoE protein was indispensable for the production of apoE-rich large HDL particles found in wild-type mice. In addition, FPLC analysis revealed that the increased free cholesterol was mainly due to the increased free cholesterol in VLDL fractions.

The analyses of hepatic lipids in apoE-deficient mice revealed a significant increase in both free cholesterol and cholesteryl ester contents with NPC1L1 expression (Fig. 3D), whereas those increases were not significant in wild-type mice. In addition, increased plasma glutamic pyruvic transaminase (GPT) levels and prominent infiltration of neutrophils in the liver specimens were found in apoE-deficient mice with NPC1L1 expression (Fig. 3E, supplementary Fig. VIII), findings not observed in C57BL/6 mice. These results suggested that ERL facilitates the secretion of free cholesterol into the circulation, thereby reducing the hepatic injury that can result from excessive accumulation of free cholesterol in the liver.

Decreased VLDL-TG production and MTP expression by hepatic NPC1L1

As described above, the neutral lipid content of pre-β lipoproteins was reduced in wild-type mice expressing NPC1L1 (Fig. 2E), whereas no reduction in VLDL cholesterol was observed (Fig. 2C). Thus, we next analyzed the changes in triglyceride metabolism induced by NPC1L1 expression. As shown in **Fig. 4A**, plasma triglyceride levels were decreased in L1-mice, and FPLC analysis revealed that this decrease was attributed to a reduction in VLDL-TG contents (Fig. 4B). These triglyceride changes were also observed in apoE-deficient mice (supplementary Fig. IX-A, B).

To illustrate the underlying mechanism behind the decrease in VLDL-TG levels, a hepatic VLDL-TG production assay was performed utilizing tyloxapol, and the reduced production of VLDL-TG was confirmed in L1-mice (Fig. 4C). One of the key molecules involved in the maturation and secretion of VLDL is the microsomal triglyceride transfer protein (MTP); consequently, we analyzed hepatic MTP expression. Compared with Null-mice without ezetimibe treatment [EZ(−)], the expression of MTP decreased by 67% in L1-EZ(−), and MTP mRNA levels in Null-EZ(+) mice were also significantly suppressed (Fig. 4D). In apoE-deficient mice infected with Ad-L1, hepatic MTP expression was also suppressed (supplementary Fig. IX-C). The decreased VLDL-TG secretion might increase hepatic triglyceride content; however, as shown in Fig. 4F, no significant difference was observed in this content. Concordant with this observation, the expression of fatty acid synthase (FAS), an important enzyme for lipogenesis, was suppressed in L1-mice (Fig. 4E).

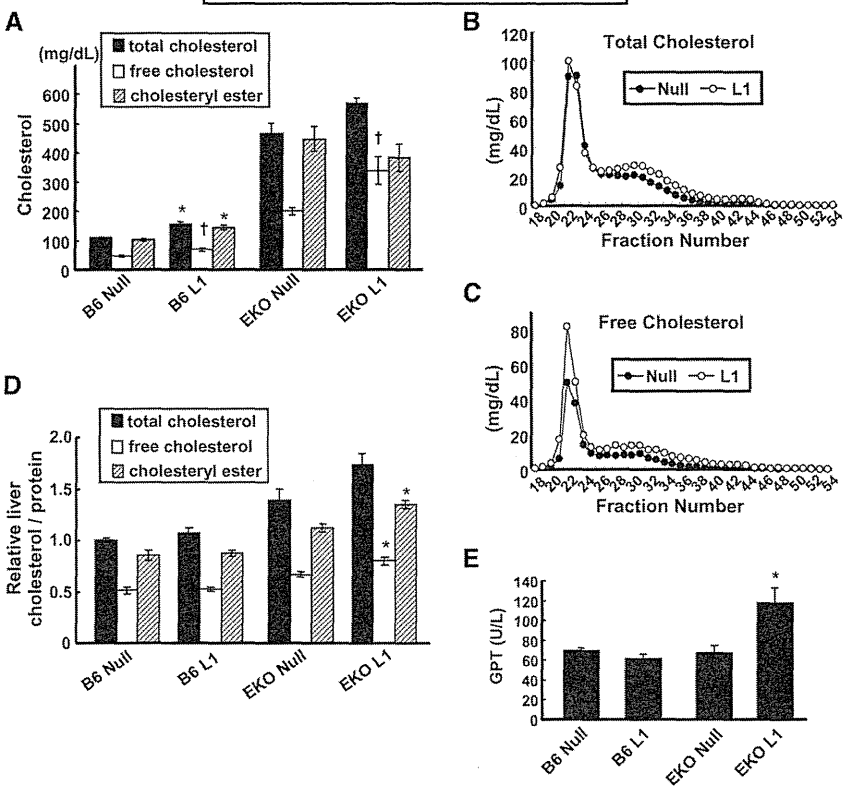

Fig. 3. Indispensable role of apoE protein in the formation of ERLs and the physiological role of ERLs in hepatic cholesterol contents and injury. Plasma and liver samples of C57BL/6 mice (B6) and apoE-deficient mice (EKO) were obtained 5 days after administration of Ad-L1 (L1) or Ad-Null (Null) (n = 3–4/each group). (A) Plasma cholesterol levels. $*P < 0.01$ and $^{\dagger}P < 0.05$ compared with Null in each group. (B, C) FPLC total (B) and free (C) cholesterol profiles of pooled plasma samples from EKO. (D) Hepatic cholesterol contents adjusted with hepatic protein levels. Data were standardized with the total cholesterol level of B6-Null. $*P < 0.01$ compared with EKO-Null mice. (E) Plasma GPT levels. $*P < 0.05$ compared with EKO-Null.

Another plausible mechanism that affects hepatic VLDL production is the increment of hepatic endoreticulum (ER) stress; a previous study indicated that hepatic ER stress destabilized apoB (23), leading to a decreased hepatic production of VLDL. Furthermore, loading of free cholesterol in some cells has been known to evoke ER stress. However, in our study, examination of X-box binding protein-1 (XBP-1) splicing and Grp78 expression, which should be modulated by hepatic ER stress, did not show any changes in these markers with NPC1L1 expression (Fig. 4G, H).

Suppression of hepatic FoxO1 protein levels with hepatic NPC1L1 expression

Because previous studies have indicated that hepatic MTP expression was negatively regulated by SREBP-1, SREBP-2 (24), and ERK activation (25) and positively regulated by forkhead box protein O1 (FoxO1) protein (26), we analyzed these factors. As shown in **Fig. 5A**, B, the nuclear protein level of SREBP-1 was not altered and that of SREBP-2 tended to be reduced in L1-mice, and no appreciable difference was observed in the extent of ERK phosphorylation between L1-EZ(–) mice and Null-EZ(–) mice. These results indicated that SREBPs and ERK might not be involved in the suppression of MTP in L1-mice. The levels of ERK phosphorylation tended to increase in mice treated with ezetimibe, suggesting that ERK activation may be one of the factors suppressing MTP in mice treated with ezetimibe. On the other hand, the FoxO1 protein level was markedly reduced in L1-mice, and this reduction was partially reversed by ezetimibe treatment (Fig. 5B), suggesting that decreased VLDL-TG production with hepatic NPC1L1 expression can be attributed to the suppression of FoxO1 protein levels.

Differential properties of cholesterol derived from bile or de novo synthesis

As described above, hepatic expression of NPC1L1 resulted in the appearance of ERL and decreased VLDL-TG production. Next, we investigated whether these metabolic changes would also be observed in experimental models of enhanced hepatic de novo cholesterol synthesis by overexpressing lanosterol synthase (LSS), an enzyme involved in cholesterol synthesis. Overexpression of LSS increased hepatic cholesterol ester contents, plasma apoB levels, and LDL cholesterol levels, accompanied by the decreased

JOURNAL OF LIPID RESEARCH ASBMB JLR

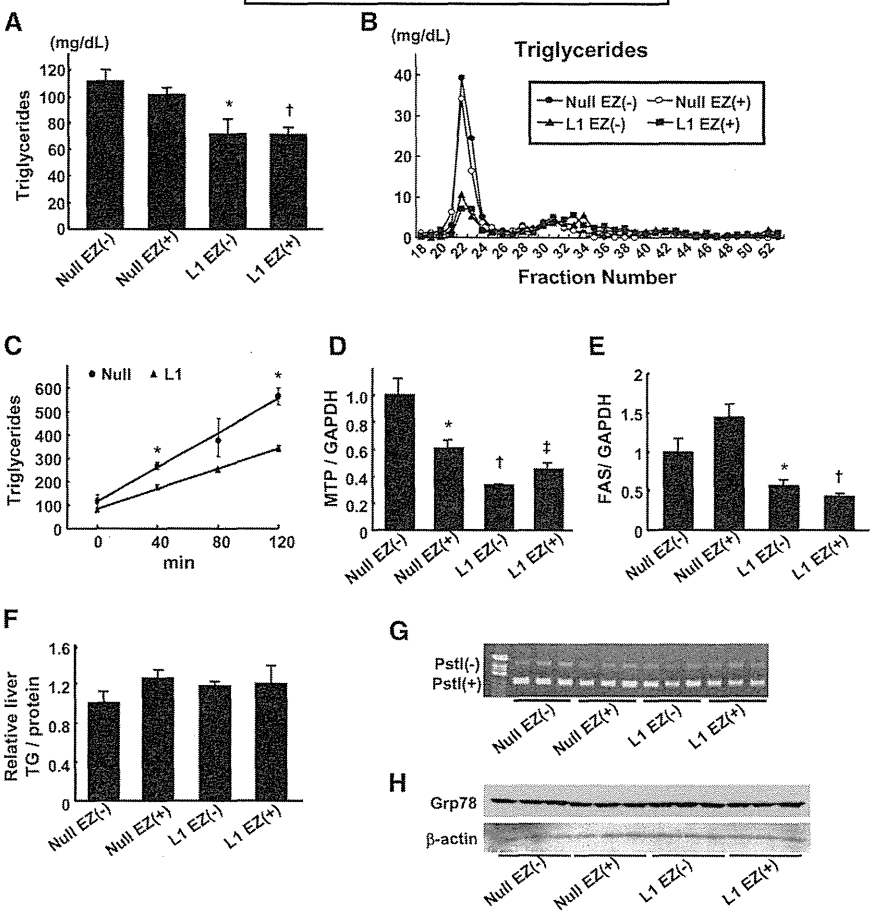

Fig. 4. Hepatic NPC1L1 overexpression decreased VLDL-TG production through the suppression of hepatic MTP expression. L1-mice and Null-mice, described in Fig. 2, were analyzed for triglyceride metabolism (n = 3–5/each group). (A) Plasma triglyceride levels. $^{*}P < 0.05$ versus Null EZ(−); $^{\dagger}P < 0.05$ versus Null EZ(−) and Null EZ(+). (B) FPLC plasma triglycerides profile. (C) VLDL-TG production assay. $^{*}P < 0.01$ compared with L1 at the same point in time. (n = 3/each group). (D, E) Hepatic MTP (D) and FAS (E) mRNA levels analyzed with real-time PCR. GAPDH was utilized as a control. (D) $^{*}P < 0.05$ compared with Null EZ(−); $^{\dagger}P < 0.01$ compared with Null EZ(−) and $P < 0.05$ compared with Null EZ(+); $^{\ddagger}P < 0.01$ compared with Null EZ(−). (E) $^{*}P < 0.01$ compared with Null EZ(+); $^{\dagger}P < 0.01$ compared with Null EZ(+), and $P < 0.05$ compared with Null EZ(−). (F) The hepatic triglyceride contents adjusted with hepatic protein levels. (G, H) Evaluation of hepatic ER stress. (G) XBP-1 splicing levels. (H) The protein expression of Grp78. β-actin was used as a control.

LDL receptor levels; however, ERLs were not found and no changes were observed in FoxO1 protein levels and VLDL-TG production rates (**Fig. 6A**, B, supplementary Fig. X).

We also examined whether the cholesterol absorbed through NPC1L1 possessed different properties compared with that synthesized de novo, utilizing HepG2 cells as in vitro models. As shown in Fig. 6C, NPC1L1 expression reduced FoxO1 protein levels in HepG2 cells, a result in accordance with that found in in vivo analysis. To analyze the effect of de novo synthesized cholesterol, we treated HepG2 cells with pitavastatin alone (p-Hep) or with pitavastatin together with mevalonate (m-Hep). As shown in Fig. 6D, E, m-Hep accumulated more cholesterol in the cells than p-Hep; however, no difference was observed in FoxO1 protein levels between p-Hep and m-Hep. These results suggested that cholesterol absorbed by NPC1L1 possessed distinct physiological properties from that derived from de novo synthesis.

DISCUSSION

In this study, we investigated the effects of hepatic NPC1L1 expression on lipoprotein metabolism and analyzed the difference in effects between cholesterol absorbed from the bile and cholesterol synthesized de novo. A previous study utilizing liver-specific NPC1L1 transgenic mice proved that hepatic NPC1L1 played a role in the absorption of cholesterol from the bile (12); however, inbred expression of NPC1L1 might provoke secondary modifications in the regulation of several genes to maintain

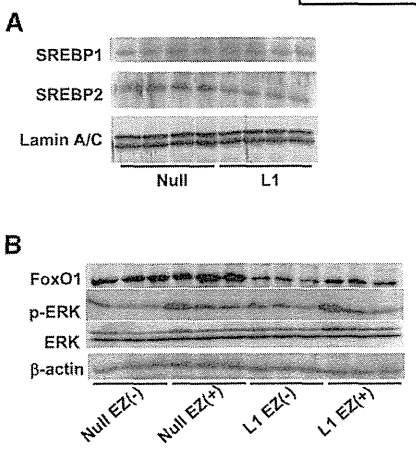

Fig. 5. Hepatic NPC1L1 reduced hepatic FoxO1 protein level. L1-mice and Null-mice, described in Fig. 2, were analyzed for proteins related with MTP expression (n = 3–5/each group). (A) Hepatic nuclear protein levels of SREBP1 and SREBP2. Lamin A/C was used as a control. (B) Western blot analyses for FoxO1, p-ERK, and ERK utilizing hepatic whole proteins. β-actin was used as a control.

homeostasis, thereby obscuring the direct effects of NPC1L1 expression. Thus, in this study, utilizing an adenoviral vector, we adventitiously expressed NPC1L1 in mice liver to elucidate the genuine effects caused by hepatic NPC1L1 expression. As shown in the results, the NPC1L1 protein expressed with adenoviral vector was localized on the side of the bile duct canaliculi, leading to the reduced cholesterol contents in the bile. With this model, we found two notable metabolic changes: the appearance of ERL in the plasma and the decrement in VLDL-TG levels.

ERLs, with particle sizes between those of LDL and HDL, would be classified as large HDL based on their mobility on agarose electrophoresis and the lack of apoB protein in the particles. Treatment with ezetimibe reduced the amount of ERLs, and the expression of LSS, an enzyme that increased cellular cholesterol content through a mechanism other than NPC1L1, did not result in the emergence of ERLs. These results indicated that hepatic NPC1L1 expression and subsequent uptake of cholesterol from the bile were essential in the appearance of ERLs. The selective uptake of free cholesterol by NPC1L1 (27) would have conferred these ERLs a unique property that they were rich in free cholesterol; this property would have been augmented by the inefficient lecithin-cholesterol acyltransferase (LCAT) function on these ERLs due to their little abundance of apolipoprotein A-I, an activator of LCAT. Furthermore, NPC1L1 expression in apoE-deficient mice did not culminate in the appearance of large HDL, suggesting that apoE protein was indispensible in the formation of ERLs. Neither the upregulation of ABCA1 protein levels, which was assumed to be responsible for the appearance of ERLs in high-cholesterol-fed NPC1L1 transgenic mice (12), nor the increased apoE expression were observed in our NPC1L1 overexpressed mice. There remains a possibility that some other factors might have

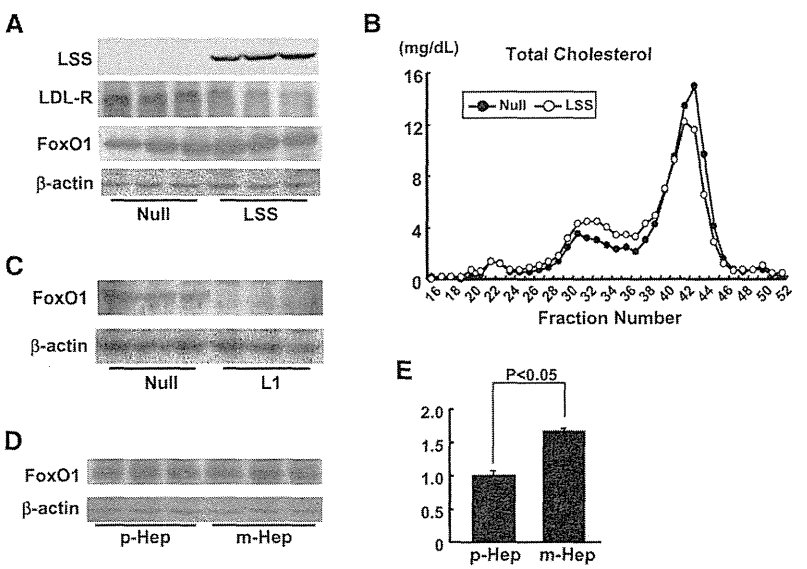

Fig. 6. The physiological consequences induced by LSS overexpression in vivo and in vitro differed from those induced by NPC1L1 overexpression. (A, B) Liver and plasma samples of C57BL/6 mice were obtained 5 days after administration of Ad-LSS (LSS) or Ad-Null (Null) (n = 3/each group). (A) Hepatic whole proteins were subjected to Western blot analyses for LSS, LDL receptor, and FoxO1 proteins. As a control, β-actin was used. (B) FPLC cholesterol profile of pooled plasma samples. (C) HepG2 cells, infected with Ad-L1 (L1) or Ad-Null (Null), were treated with bile micelles, and FoxO1 protein level was determined (n = 3). As a control, β-actin was used. (D, E) HepG2 cells were treated with pitavastatin alone (p-Hep) or with both pitavastatin and mevalonate (m-Hep) for 24 h (n = 3). (D) FoxO1 protein levels. (E) The cellular cholesterol contents adjusted by cellular protein levels.

JOURNAL OF LIPID RESEARCH ASBMB

contributed to the formation or the appearance of ERLs. For example, the clearance of ERLs might be retarded, considering the decreased protein level of LDL receptor and the decreased chylomicron clearance; or, the activities of lipases might be modulated, resulting in the increased plasma ERL levels. However, in light of the findings that the free cholesterol content of ERLs was much higher on day 3 (supplementary Fig. XI) than on day 5 and that ERLs were produced by HepG2 cells overexpressing NPC1L1, it can be speculated that ERLs were formed as a direct consequence of the increased cholesterol uptake from the bile.

ERLs are usually not detected in the plasma of normal humans who express NPC1L1 in the liver. However, expression of NPC1L1 in mice liver resulted in the emergence of these unique lipoproteins. The possible explanation for the appearance of ERLs in L1-mice may be that the mice are deficient in cholesteryl ester transfer protein (CETP). In fact, it was reported that subjects with CETP deficiency have apoE-rich HDL (28) and that pharmacological inhibition of CETP resulted in the increment of plasma apoE levels, especially in HDL fractions (29). Furthermore, expression of CETP in SR-BI-deficient mice, the animal model which possesses ERLs in the plasma, resulted in the reduction of ERL levels (30, 31). Of course, the extent to which hepatic ERL production contributes to the increase of apoE-rich HDL under CETP inhibition is still unclear; further analyses are awaited to clarify the association of CETP and the appearance of ERLs.

ApoE-deficient mice, which did not produce ERLs due to the lack of apoE, manifested hepatic injury upon NPC1L1 expression. Thus, one of the physiological roles of ERLs is to ameliorate hepatic injury that results from excessive free cholesterol taken up by the bile. In addition, as demonstrated in previous reports, HDLs abundant in apoE, regardless of its isoform, facilitated reverse cholesterol transport, thereby possibly exerting an antiatherogenic function (32, 33). Future investigations are necessary to test whether the ERLs produced directly from the liver possess antiatherogenic functions should CETP inhibitors become promising antidyslipidemic agents (34, 35).

The other consequence of hepatic NPC1L1 expression on lipid metabolism was the drop in plasma triglyceride levels due to the suppression of VLDL-TG production. This decrease in VLDL-TG production was, at least in part, attributed to the reduced expression of MTP, and the decreased MTP expression was assumed to be the consequence of the reduction in FoxO1 protein levels. Because FoxO1 protein is a transcriptional factor that plays an important role not only in lipid metabolism but also in glucose metabolism (26, 36, 37), further investigation on glucose metabolism in our present model might be fascinating.

The expression of NPC1L1 in the liver facilitates cholesterol uptake from the bile, whereas ezetimibe treatment inhibits cholesterol uptake from the bile. Thus, our observation of plasma triglycerides levels in L1-mice appears to be inconsistent with the previous reports demonstrating that administration of ezetimibe ameliorated triglyceride metabolism in rats (38) and decreased plasma TG levels in humans (3, 5, 6). A probable explanation for this discrepancy is that the levels of hepatic NPC1L1 expression in our model were so high that the delicate physiological balance between hepatic and intestinal NPC1L1 functions had been disturbed. In fact, as shown in Fig. 4D, ezetimibe treatment in Null-mice did decrease hepatic MTP expression. Taking account of these results and speculations, selective inhibition of intestinal NPC1L1 might be more beneficial in reducing plasma TG levels.

Through this study, we found that, depending on its source of origin, cholesterol exerts a differential effect on the intracellular metabolism. Both the NPC1L1 expression and LSS expression resulted in increased intracellular cholesterol levels; however, the former resulted in the plasma appearance of ERLs and suppression of FoxO1, while the latter did not. One possible explanation for this difference is the different localization of cholesterol originating from different sources: cholesterol taken up by NPC1L1 is delivered to the early endosome after being incorporated to the plasma membrane, whereas cholesterol synthesized de novo is localized on the ER membrane. It is easy to speculate that this different localization of cholesterol in the cellular organelle induces the subsequent differential physiological effect, thereby affecting the plasma lipoprotein metabolism. Considering that cholesterol in apoB-containing lipoproteins is taken up through lipoprotein receptors and undergoes lysosomal processing, it is possible that cholesterol derived from lipoproteins may possess unique properties. Future investigation of the intracellular transport pathways of cholesterol derived from different sources and their metabolic effects would enrich our understanding of the hepatic cholesterol metabolism and perhaps culminate in the development of a better treatment strategy for dyslipidemia and atherosclerosis.

In summary, the hepatic expression of NPC1L1 in mice resulted in the plasma appearance of ERLs and the decrement of VLDL-TG secreted from the liver. These findings were not found in mice with increased hepatic de novo cholesterol synthesis, suggesting that cholesterol, depending on its source, exerted distinct properties in cellular and plasma lipid metabolism.

REFERENCES

1. Rosenblum, S. B., T. Huynh, A. Afonso, H. R. Davis, Jr., N. Yumibe, J. W. Clader, and D. A. Burnett. 1998. Discovery of 1-(4-fluorophenyl)-(3R)-[3-(4-fluorophenyl)-(3S)-hydroxypropyl]-(4S)-(4 -hydroxyphenyl)-2-azetidinone (SCH 58235): a designed, potent, orally active inhibitor of cholesterol absorption. *J. Med. Chem.* **41:** 973–980.
2. Bays, H. E., P. B. Moore, M. A. Drehobl, S. Rosenblatt, P. D. Toth, C. A. Dujovne, R. H. Knopp, L. J. Lipka, A. P. Lebeaut, B. Yang, et al. 2001. Effectiveness and tolerability of ezetimibe in patients with primary hypercholesterolemia: pooled analysis of two phase II studies. *Clin. Ther.* **23:** 1209–1230.
3. Dujovne, C. A., M. P. Ettinger, J. F. McNeer, L. J. Lipka, A. P. LeBeaut, R. Suresh, B. Yang, and E. P. Veltri. 2002. Efficacy and safety of a potent new selective cholesterol absorption inhibitor, ezetimibe, in patients with primary hypercholesterolemia. *Am. J. Cardiol.* **90:** 1092–1097.
4. Knopp, R. H., H. Gitter, T. Truitt, H. Bays, C. V. Manion, L. J. Lipka, A. P. LeBeaut, R. Suresh, B. Yang, and E. P. Veltri. 2003. Effects of

ezetimibe, a new cholesterol absorption inhibitor, on plasma lipids in patients with primary hypercholesterolemia. *Eur. Heart J.* **24:** 729–741.

5. Pandor, A., R. M. Ara, I. Tumur, A. J. Wilkinson, S. Paisley, A. Duenas, P. N. Durrington, and J. Chilcott. 2009. Ezetimibe monotherapy for cholesterol lowering in 2,722 people: systematic review and meta-analysis of randomized controlled trials. *J. Intern. Med.* **265:** 568–580.
6. Masuda, D., Y. Nakagawa-Toyama, K. Nakatani, M. Inagaki, K. Tsubakio-Yamamoto, J. C. Sandoval, T. Ohama, M. Nishida, M. Ishigami, and S. Yamashita. 2009. Ezetimibe improves postprandial hyperlipidaemia in patients with type IIb hyperlipidaemia. *Eur. J. Clin. Invest.* **39:** 689–698.
7. Altmann, S. W., H. R. Davis, Jr., L. J. Zhu, X. Yao, L. M. Hoos, G. Tetzloff, S. P. Iyer, M. Maguire, A. Golovko, M. Zeng, et al. 2004. Niemann-Pick C1 Like 1 protein is critical for intestinal cholesterol absorption. *Science.* **303:** 1201–1204.
8. Davis, H. R., Jr., L. J. Zhu, L. M. Hoos, G. Tetzloff, M. Maguire, J. Liu, X. Yao, S. P. Iyer, M. H. Lam, E. G. Lund, et al. 2004. Niemann-Pick C1 Like 1 (NPC1L1) is the intestinal phytosterol and cholesterol transporter and a key modulator of whole-body cholesterol homeostasis. *J. Biol. Chem.* **279:** 33586–33592.
9. Yu, L., S. Bharadwaj, J. M. Brown, Y. Ma, W. Du, M. A. Davis, P. Michaely, P. Liu, M. C. Willingham, and L. L. Rudel. 2006. Cholesterol-regulated translocation of NPC1L1 to the cell surface facilitates free cholesterol uptake. *J. Biol. Chem.* **281:** 6616–6624.
10. Yamanashi, Y., T. Takada, and H. Suzuki. 2007. Niemann-Pick C1-like 1 overexpression facilitates ezetimibe-sensitive cholesterol and beta-sitosterol uptake in CaCo-2 cells. *J. Pharmacol. Exp. Ther.* **320:** 559–564.
11. Ge, L., J. Wang, W. Qi, H. H. Miao, J. Cao, Y. X. Qu, B. L. Li, and B. L. Song. 2008. The cholesterol absorption inhibitor ezetimibe acts by blocking the sterol-induced internalization of NPC1L1. *Cell Metab.* **7:** 508–519.
12. Temel, R. E., W. Tang, Y. Ma, L. L. Rudel, M. C. Willingham, Y. A. Ioannou, J. P. Davies, L. M. Nilsson, and L. Yu. 2007. Hepatic Niemann-Pick C1-like 1 regulates biliary cholesterol concentration and is a target of ezetimibe. *J. Clin. Invest.* **117:** 1968–1978.
13. Wiersma, H., A. Gatti, N. Nijstad, F. Kuipers, and U. J. Tietge. 2009. Hepatic SR-BI, not endothelial lipase, expression determines biliary cholesterol secretion in mice. *J. Lipid Res.* **50:** 1571–1580.
14. Wiersma, H., A. Gatti, N. Nijstad, R. P. Oude Elferink, F. Kuipers, and U. J. Tietge. 2009. Scavenger receptor class B type I mediates biliary cholesterol secretion independent of ATP-binding cassette transporter g5/g8 in mice. *Hepatology.* **50:** 1263–1272.
15. Narushima, K., T. Takada, Y. Yamanashi, and H. Suzuki. 2008. Niemann-pick C1-like 1 mediates alpha-tocopherol transport. *Mol. Pharmacol.* **74:** 42–49.
16. Labonté, E. D., L. M. Camarota, J. C. Rojas, R. J. Jandacek, D. E. Gilham, J. P. Davies, Y. A. Ioannou, P. Tso, D. Y. Hui, and P. N. Howles. 2008. Reduced absorption of saturated fatty acids and resistance to diet-induced obesity and diabetes by ezetimibe-treated and Npc1l1-/- mice. *Am. J. Physiol. Gastrointest. Liver Physiol.* **295:** G776–G783.
17. Kurano, M., N. Iso-O, M. Hara, E. Noiri, K. Koike, T. Kadowaki, and K. Tsukamoto. 2011. Plant sterols increased IL-6 and TNF-alpha secretion from macrophages, but to a lesser extent than cholesterol. *J. Atheroscler. Thromb.* **18:** 373–383.
18. Kurano, M., N. Iso-O, M. Hara, N. Ishizaka, K. Moriya, K. Koike, and K. Tsukamoto. 2011. LXR agonist increases apoE secretion from HepG2 spheroid, together with an increased production of VLDL and apoE-rich large HDL. *Lipids Health Dis.* **10:** 134.
19. Tsukamoto, K., C. Maugeais, J. M. Glick, and D. J. Rader. 2000. Markedly increased secretion of VLDL triglycerides induced by gene transfer of apolipoprotein E isoforms in apoE-deficient mice. *J. Lipid Res.* **41:** 253–259.
20. Krimbou, L., M. Tremblay, J. Davignon, and J. S. Cohn. 1997. Characterization of human plasma apolipoprotein E-containing lipoproteins in the high density lipoprotein size range: focus on pre-beta1-LpE, pre-beta2-LpE, and alpha-LpE. *J. Lipid Res.* **38:** 35–48.
21. Krimbou, L., M. Marcil, H. Chiba, and J. Genest, Jr. 2003. Structural and functional properties of human plasma high density-sized lipoprotein containing only apoE particles. *J. Lipid Res.* **44:** 884–892.
22. Vaisman, B. L., G. Lambert, M. Amar, C. Joyce, T. Ito, R. D. Shamburek, W. J. Cain, J. Fruchart-Najib, E. D. Neufeld, A. T. Remaley, et al. 2001. ABCA1 overexpression leads to hyperalphalipoproteinemia and increased biliary cholesterol excretion in transgenic mice. *J. Clin. Invest.* **108:** 303–309.
23. Ota, T., C. Gayet, and H. N. Ginsberg. 2008. Inhibition of apolipoprotein B100 secretion by lipid-induced hepatic endoplasmic reticulum stress in rodents. *J. Clin. Invest.* **118:** 316–332.
24. Sato, R., W. Miyamoto, J. Inoue, T. Terada, T. Imanaka, and M. Maeda. 1999. Sterol regulatory element-binding protein negatively regulates microsomal triglyceride transfer protein gene transcription. *J. Biol. Chem.* **274:** 24714–24720.
25. Au, W. S., H. F. Kung, and M. C. Lin. 2003. Regulation of microsomal triglyceride transfer protein gene by insulin in HepG2 cells: roles of MAPKerk and MAPKp38. *Diabetes.* **52:** 1073–1080.
26. Kamagate, A., and H. H. Dong. 2008. FoxO1 integrates insulin signaling to VLDL production. *Cell Cycle.* **7:** 3162–3170.
27. Brown, J. M., L. L. Rudel, and L. Yu. 2007. NPC1L1 (Niemann-Pick C1-like 1) mediates sterol-specific unidirectional transport of non-esterified cholesterol in McArdle-RH7777 hepatoma cells. *Biochem. J.* **406:** 273–283.
28. Yamashita, S., D. L. Sprecher, N. Sakai, Y. Matsuzawa, S. Tarui, and D. Y. Hui. 1990. Accumulation of apolipoprotein E-rich high density lipoproteins in hyperalphalipoproteinemic human subjects with plasma cholesteryl ester transfer protein deficiency. *J. Clin. Invest.* **86:** 688–695.
29. Zhang, B., P. Fan, E. Shimoji, H. Xu, K. Takeuchi, C. Bian, and K. Saku. 2004. Inhibition of cholesteryl ester transfer protein activity by JTT-705 increases apolipoprotein E-containing high-density lipoprotein and favorably affects the function and enzyme composition of high-density lipoprotein in rabbits. *Arterioscler. Thromb. Vasc. Biol.* **24:** 1910–1915.
30. Rigotti, A., B. L. Trigatti, M. Penman, H. Rayburn, J. Herz, and M. Krieger. 1997. A targeted mutation in the murine gene encoding the high density lipoprotein (HDL) receptor scavenger receptor class B type I reveals its key role in HDL metabolism. *Proc. Natl. Acad. Sci. USA.* **94:** 12610–12615.
31. Hildebrand, R. B., B. Lammers, I. Meurs, S. J. Korporaal, W. De Haan, Y. Zhao, J. K. Kruijt, D. Pratico, A. W. Schimmel, A. G. Holleboom, et al. 2010. Restoration of high-density lipoprotein levels by cholesteryl ester transfer protein expression in scavenger receptor class B type I (SR-BI) knockout mice does not normalize pathologies associated with SR-BI deficiency. *Arterioscler. Thromb. Vasc. Biol.* **30:** 1439–1445.
32. Matsuura, F., N. Wang, W. Chen, X. C. Jiang, and A. R. Tall. 2006. HDL from CETP-deficient subjects shows enhanced ability to promote cholesterol efflux from macrophages in an apoE- and ABCG1-dependent pathway. *J. Clin. Invest.* **116:** 1435–1442.
33. Hara, M., T. Matsushima, H. Satoh, N. Iso-o, H. Noto, M. Togo, S. Kimura, Y. Hashimoto, and K. Tsukamoto. 2003. Isoform-dependent cholesterol efflux from macrophages by apolipoprotein E is modulated by cell surface proteoglycans. *Arterioscler. Thromb. Vasc. Biol.* **23:** 269–274.
34. Davidson, M. H. 2010. Update on CETP inhibition. *J. Clin. Lipidol.* **4:** 394–398.
35. Cannon, C. P., S. Shah, H. M. Dansky, M. Davidson, E. A. Brinton, A. M. Gotto, M. Stepanavage, S. X. Liu, P. Gibbons, T. B. Ashraf, et al. 2010. Safety of anacetrapib in patients with or at high risk for coronary heart disease. *N. Engl. J. Med.* **363:** 2406–2415.
36. Nakae, J., T. Kitamura, D. L. Silver, and D. Accili. 2001. The forkhead transcription factor Foxo1 (Fkhr) confers insulin sensitivity onto glucose-6-phosphatase expression. *J. Clin. Invest.* **108:** 1359–1367.
37. Zhang, W., S. Patil, B. Chauhan, S. Guo, D. R. Powell, J. Le, A. Klotsas, R. Matika, X. Xiao, R. Franks, et al. 2006. FoxO1 regulates multiple metabolic pathways in the liver: effects on gluconeogenic, glycolytic, and lipogenic gene expression. *J. Biol. Chem.* **281:** 10105–10117.
38. Nomura, M., H. Ishii, A. Kawakami, and M. Yoshida. 2009. Inhibition of Hepatic Neiman-Pick C1-Like 1 improves hepatic insulin resistance. *Am. J. Physiol. Endocrinol. Metab.* **297:** E1030–E1038.

HEPATOLOGY
Official Journal of the American Association for the Study of Liver Diseases

MicroRNA-140 Acts as a Liver Tumor Suppressor by Controlling NF-κB Activity by Directly Targeting DNa Methyltransferase 1 (Dnmt1) Expression

Akemi Takata,[1] Motoyuki Otsuka,[1] Takeshi Yoshikawa,[1] Takahiro Kishikawa,[1] Yohko Hikiba,[2] Shuntaro Obi,[3] Tadashi Goto,[1] Young Jun Kang,[4] Shin Maeda,[1] Haruhiko Yoshida,[1] Masao Omata,[1] Hiroshi Asahara,[5,6,7] and Kazuhiko Koike[1]

MicroRNAs (miRNAs) are small RNAs that regulate the expression of specific target genes. While deregulated miRNA expression levels have been detected in many tumors, whether miRNA functional impairment is also involved in carcinogenesis remains unknown. We investigated whether deregulation of miRNA machinery components and subsequent functional impairment of miRNAs are involved in hepatocarcinogenesis. Among miRNA-containing ribonucleoprotein complex components, reduced expression of DDX20 was frequently observed in human hepatocellular carcinomas, in which enhanced nuclear factor-κB (NF-κB) activity is believed to be closely linked to carcinogenesis. Because DDX20 normally suppresses NF-κB activity by preferentially regulating the function of the NF-κB-suppressing miRNA-140, we hypothesized that impairment of miRNA-140 function may be involved in hepatocarcinogenesis. DNA methyltransferase 1 (Dnmt1) was identified as a direct target of miRNA-140, and increased Dnmt1 expression in DDX20-deficient cells hypermethylated the promoters of metallothionein genes, resulting in decreased metallothionein expression leading to enhanced NF-κB activity. MiRNA-140-knockout mice were prone to hepatocarcinogenesis and had a phenotype similar to that of DDX20 deficiency, suggesting that miRNA-140 plays a central role in DDX20 deficiency-related pathogenesis. *Conclusion*: These results indicate that miRNA-140 acts as a liver tumor suppressor, and that impairment of miRNA-140 function due to a deficiency of DDX20, a miRNA machinery component, could lead to hepatocarcinogenesis. (HEPATOLOGY 2013;57:162-170)

Hepatocellular carcinoma (HCC) is the third most common cause of cancer-related mortality worldwide.[1] Although multiple major risk factors have been identified, such as infection with hepatitis viruses B or C, the molecular mechanisms underlying HCC development remain poorly understood, hindering the development of novel therapeutic approaches. Therefore, a better understanding of the molecular pathways involved in hepatocarcinogenesis is critical for the development of new therapeutic options.

Nuclear factor-κB (NF-κB) is one of the best-characterized intracellular signaling pathways. Its activation is a common feature of human HCC.[2-4] It acts as an inhibitor of apoptosis and as a tumor promoter[4,5] and is associated with the acquisition of a transformed phenotype during hepatocarcinogenesis.[6] In fact, studies using patient samples suggest that NF-κB activation in the liver leads to the development of HCC.[7] Although there are conflicting reports,[8] activation of the NF-κB pathway in the liver is crucial for the initiation and promotion of HCC.[4]

Abbreviations: DEN, diethylnitrosamine; Dnmt1, DNA methyltransferase 1; HCC, hepatocellular carcinoma; miRNA; microRNA; miRNP, miRNA-containing ribonucleoprotein; MT, metallothionein; NF-κB, nuclear factor-κB; RT-PCR, reverse-transcription polymerase chain reaction; TNF-α, tumor necrosis factor-α; TRAIL, TNF-related apoptosis-inducing ligand; UTR, untranslated region.

From the [1]Department of Gastroenterology, Graduate School of Medicine, The University of Tokyo, Tokyo, Japan; the [2]Division of Gastroenterology, Institute for Adult Diseases, Asahi Life Foundation, Tokyo, Japan; the [3]Department of Hepatology, Kyoundo Hospital, Tokyo, Japan; the [4]Department of Immunology and Microbial Science, and the [5]Department of Molecular and Experimental Medicine, The Scripps Research Institute, La Jolla, CA; the [6]Department of Systems BioMedicine, Tokyo Medical and Dental University, Tokyo, Japan; and [7]CREST, Japan Science and Technology Agency, Tokyo, Japan.

Received March 30, 2012; accepted July 18, 2012.

Supported by Grants-in-Aid from the Ministry of Education, Culture, Sports, Science and Technology, Japan (#22390058, #23590960, and #20390204) (M. O., T. G., and K. K.); Health Sciences Research Grants from the Ministry of Health, Labor and Welfare of Japan (Research on Hepatitis) (to K. K.); National Institutes of Health Grant R01AI088229 (to Y. J. K.); the Miyakawa Memorial Research Foundation (to A. T.); and grants from the Sagawa Foundation for Promotion of Cancer Research, the Astellas Foundation for Research on Metabolic Disorders, and the Cell Science Research Foundation (to M. O.).

MicroRNAs (miRNAs) are small RNA molecules that regulate the expression of target genes and are involved in various biological functions.[9-12] Although specific miRNAs can function as either suppressors or oncogenes in tumor development, a general reduction in miRNA expression is commonly observed in human cancers.[13-22] In this context, it can be hypothesized that deregulation of the machinery components involved in miRNA function may be related to the functional impairment of miRNAs and the pathogenesis of carcinogenesis.

In this study, we show that the expression of DDX20, an miRNA-containing ribonucleoprotein (miRNP) component, is frequently decreased in human HCC. Because DDX20 is required for both the preferential loading of miRNA-140 into the RNA-induced silencing complex and its function,[23] we hypothesized that DDX20 deficiency would lead to hepatocarcinogenesis via impaired miRNA-140 function. MiRNA-140 knockout mice were indeed more prone to hepatocarcinogenesis, and we identified a possible molecular pathway from DDX20 deficiency to liver cancer.

Materials and Methods

Mouse and Liver Tumor Induction. MiRNA-140$^{-/-}$ mice have been described.[24] Recombinant murine tumor necrosis factor-α (TNF-α) (25 μg/kg; Wako, Osaka, Japan) was injected into the tail vein, and the mice were sacrificed 1 hour later. To induce liver tumors, 15-day-old mice received an intraperitoneal injection of diethylnitrosamine (DEN) (25 mg/kg body weight), and were sacrificed 32 weeks later. All animal experiments were performed in compliance with the regulations of the Animal Use Committee of the University of Tokyo and the Institute for Adult Disease, Asahi Life Foundation.

Plasmids. FLAG-tagged human DDX20-expressing plasmids were as described.[23] The pGL3-based reporter plasmid containing Dnmt1 3′ untranslated region (UTR) sequences was provided by G. Marucucci.[25]

Detailed Materials and Methods. The detailed experimental procedures of clinical samples, cells, plasmids, reporter assays, reverse-transcription polymerase chain reaction (RT-PCR) analysis, antibodies, western blotting, cell assays, immunohistochemistry, microarray analysis, methylation analysis, and electrophoretic mobility-shift assay are described in the Supporting Information.

Statistical Analysis. Statistically significant differences between groups were determined using a Wilcoxon rank-sum test. A Wilcoxon signed-rank test was used for statistical comparisons of protein expression levels between HCC and surrounding noncancerous tissues.

Table 1. Cases with Differential Expression Levels of miRNP Components in HCC (n = 10)

Gene ID	Gene Symbol	Decreased	Increased	No Change
23405	Dicer1	2	1	7
27161	EIF2C2 (AGO2)	1	1	8
6895	TARBP2(TRBP2)	2	0	8
11218	DDX20 (GEMIN3)	8	0	2
50628	GEMIN4	1	0	9

The expression levels of each miRNP component were determined via immunohistochemistry.

The numbers indicate the number of cases that had the differential expression levels (decreased, increased, or no change) in HCC tissues compared with those in surrounding liver tissues.

Results

DDX20 Expression Is Frequently Decreased in HCC. The expression levels of proteins reported to be miRNP components (Dicer, Ago2, TRBP2, DDX20 [also known as Gemin3], and Gemin4)[26] were initially determined via immunohistochemistry in HCC and noncancerous background liver tissues from 10 patients. DDX20 expression was lower in HCC tissue compared with the surrounding noncancerous tissue in 8 of 10 cases, whereas expression of the other genes was unchanged (Table 1 and Supporting Fig. 1). Therefore, and because DDX20 was recently identified as a possible liver tumor suppressor in mice,[27] we determined its role as a human HCC suppressor.

DDX20 protein expression was lower in several HCC cell lines, such as Huh7 and Hep3B (Fig. 1A), compared with normal hepatocytes. DDX20 protein levels were also lower in human HCC needle biopsy specimens than in surrounding noncancerous liver tissue (Fig. 1B). Immunohistochemical analysis

Address reprint requests to: Motoyuki Otsuka, M.D., Department of Gastroenterology, Graduate School of Medicine, University of Tokyo, 7-3-1 Hongo, Bunkyo-ku, Tokyo 113-8655, Japan. E-mail: otsukamo-tky@umin.ac.jp; fax: (81)-3-3814-0021.

View this article online at wileyonlinelibrary.com.

DOI 10.1002/hep.26011

Potential conflict of interest: Nothing to report.

Additional Supporting Information may be found in the online version of this article.

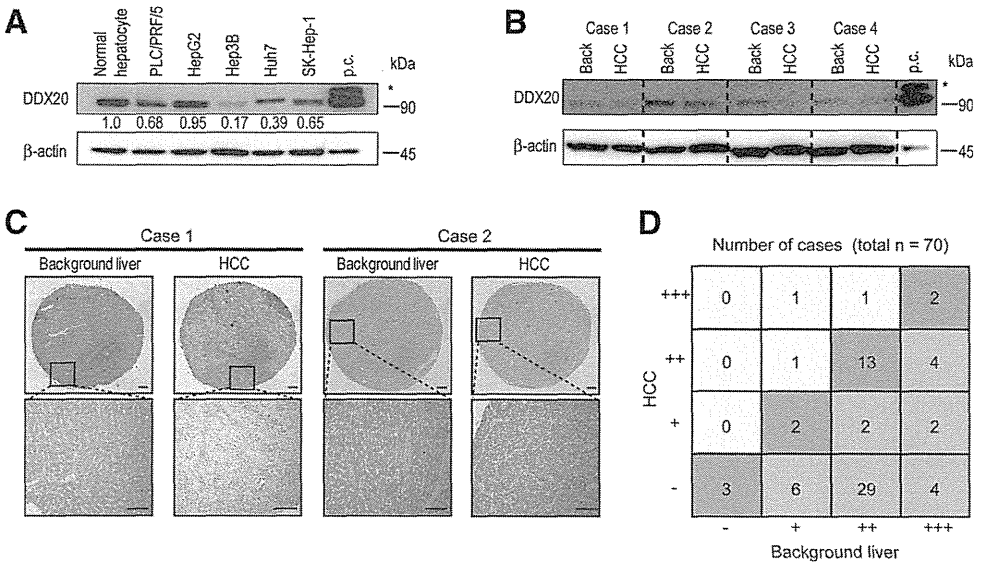

Fig. 1. Reduced DDX20 expression levels in hepatocellular carcinoma. (A) DDX20 protein expression in HCC cell lines. Numbers between the panels indicate DDX20 protein levels normalized to β-actin levels. Lysates of 293T cells transiently transfected with a FLAG-tagged DDX20-expressing plasmid yielded two DDX20 bands corresponding to the endogenous DDX20 protein and the transfected FLAG-tagged DDX20 protein (*) as a positive control (p.c.; far right lane). Data represent the results of three independent determinations. (B) DDX20 protein expression in four HCC needle biopsy specimens and in the surrounding noncancerous background liver tissue (Back). *Positive control. (C) Immunohistochemical analysis of DDX20 protein expression in HCC and surrounding tissues (background liver). Two representative cases are shown. Scale bars, 500 μm. The lower panels display magnified images of the boxed areas in the upper panels. (D) Grid summarizing DDX20 immunohistochemical staining data from 70 cases. In 47 cases (pink shading), DDX20 protein levels were lower in the HCC tissues than in the surrounding tissues ($P < 0.05$; Wilcoxon signed-rank test).

confirmed that DDX20 expression was frequently lower in HCC than in surrounding noncancerous liver tissue (Fig. 1C,D). Specifically, 47 of 70 cases examined showed reduced DDX20 protein expression in HCC versus background noncancerous liver tissue (Fig. 1D and Supporting Table 1). These results indicate that the expression of DDX20, an miRNP component, is frequently reduced in human HCC, and suggest that this reduced DDX20 expression might be involved in the pathogenesis of a subset of HCC cases.

NF-κB Activity Is Enhanced by DDX20 Deficiency. Because DDX20 knockout mice are embryonic-lethal,[28] DDX20 has been suggested to have important biological roles. DDX20, a DEAD-box protein,[29] was originally found to interact with survival motor neuron protein.[30] Later, it was identified as a major component of miRNPs,[31] which may mediate miRNA function. As we have reported, DDX20 is preferentially involved in miRNA-140-3p function,[23] acting as a suppressor of NF-κB activity in the liver.[32] DDX20-knockdown PLC/PRF/5 cells exhibit enhanced NF-κB activity[23] (Fig. 2A). Whereas the proliferation rates of DDX20-knockdown cells and control cells were comparable (Fig. 2B), apoptotic cell death after stimulation with TNF-related apoptosis-inducing ligand (TRAIL), which induces both cell apoptosis and NF-κB activation,[33] was significantly reduced in DDX20-knockdown cells (Fig. 2C). Similar results were obtained using DDX20-knockdown HepG2 cells (Supporting Fig. 2A-D). Conversely, NF-κB activity was reduced, but cell proliferation remained unchanged, in Hep3B cells stably overexpressing DDX20 (Fig. 2D,E). Sensitivity to TRAIL-induced apoptosis was restored in these cells (Fig. 2F). Similar results were also obtained using Huh7 cells (Supporting Fig. 2E-H). These data confirm a previous report that DDX20 deficiency enhances NF-κB activity and the downstream events of this pathway.

Metallothionein Expression Is Decreased by DDX20 Deficiency. Next, to investigate the biological consequences of DDX20 deficiency, we examined the changes in transcript levels in DDX20-knockdown cells using microarrays (GEO accession number: GSE28088). The expression of genes driven by NF-κB that are related to carcinogenesis, such as FASLG, IRAK1, CARD9, and Galectin-1, were enhanced significantly in DDX20-knockdown cells, as expected (Table 2). To determine the mechanism underlying the enhanced NF-κB activation in DDX20-deficient cells, we searched for candidate genes and noticed that the